

# Fine-tuning Language Models over Slow Networks using Activation Compression with Guarantees

Jue Wang<sup>†\*</sup>, Binhang Yuan<sup>†\*</sup>, Luka Rimanic<sup>†\*</sup>, Yongjun He<sup>†</sup>, Tri Dao<sup>‡</sup>,  
Beidi Chen<sup>‡</sup>, Christopher Re<sup>‡</sup>, Ce Zhang<sup>†</sup>

<sup>†</sup>ETH Zürich, Switzerland   <sup>‡</sup>Stanford University, USA  
{jue.wang, binhng.yuan, luka.rimanic, yongjun.he, ce.zhang}@inf.ethz.ch  
{beidic, trid, chrismre}@stanford.edu

## Abstract

Communication compression is a crucial technique for modern distributed learning systems to alleviate their communication bottlenecks over slower networks. Despite recent intensive studies of gradient compression for data parallel-style training, compressing the *activations* for models trained with pipeline parallelism is still an open problem. In this paper, we propose AC-SGD, a novel activation compression algorithm for communication-efficient pipeline parallelism training over slow networks. Different from previous efforts in activation compression, instead of compressing activation values directly, AC-SGD compresses the *changes of the activations*. This allows us to show, to the best of our knowledge for the first time, that one can still achieve  $O(1/\sqrt{T})$  convergence rate for non-convex objectives under activation compression, without making assumptions on gradient unbiasedness that do not hold for deep learning models with non-linear activation functions. We then show that AC-SGD can be optimized and implemented efficiently, without additional end-to-end runtime overhead. We evaluated AC-SGD to fine-tune language models with up to 1.5 billion parameters, compressing activations to 2-4 bits. AC-SGD provides up to  $4.3\times$  end-to-end speed-up in slower networks, without sacrificing model quality. Moreover, we also show that AC-SGD can be combined with state-of-the-art gradient compression algorithms to enable “end-to-end communication compression”: *All communications between machines, including model gradients, forward activations, and backward gradients are compressed into lower precision*. This provides up to  $4.9\times$  end-to-end speed-up, without sacrificing model quality.

**Code Availability:** <https://github.com/DS3Lab/AC-SGD>

## 1 Introduction

Recent efforts in improving communication efficiency for distributed learning have significantly decreased the dependency of training deep learning models on fast data center networks — the *gradient* can be compressed to lower precision or sparsified [1, 2, 3, 4], which speeds up training over low bandwidth networks, whereas the *communication topology* can be decentralized [5, 6, 7, 8, 9, 10], which speeds up training over high latency networks. Indeed, today’s state-of-the-art training systems, such as Pytorch [11, 12], Horovod [13], Bagua [14], and BytePS [15], already support many of these communication-efficient training paradigms.

However, with the rise of large foundation models [16] (e.g., BERT [17], GPT-3 [18], and CLIP[19]), improving communication efficiency via compression becomes more challenging. Current training systems for foundation models such as Megatron [20], Deepspeed [21], and FairScale [22], allocate different layers of the model onto multiple devices and need to communicate — *in addition to* the gradients on the models — the

---

\* Equal contribution.

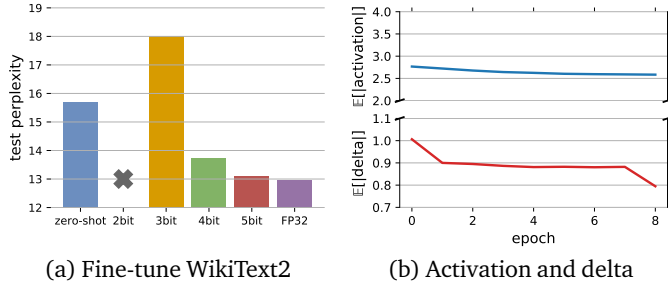


Figure 1: (a) Fine-tuning GPT2-1.5B with different activation precisions in communication; (b) Average absolute value of activations and their changes for GPT2-1.5B during training.

Algorithm	Assumptions on Quant. Grad.	Conv. Rate
SGD [25]	N/A	$\mathcal{O}(1/\sqrt{T})$
AC-GC [26]	Unbiased	$\mathcal{O}(1/\sqrt{T})$
TinyScript [27]	Unbiased	$\mathcal{O}(1/\sqrt{T})$
AC-SGD	N/A	$\mathcal{O}(1/\sqrt{T})$

Table 1: Summary of technical highlights among standard SGD, AC-GD, TinyScript and AC-SGD. AC-GC [26] and TinyScript [27] assume that the returned gradient is unbiased, whereas AC-SGD algorithm does not rely on such an assumption.

*activations* during the forward pass and the *gradients on the activations* during the backward pass. Compressing these *activations* leads to a very different behavior compared with compressing the gradient — *simply compressing these activations in a stochastically unbiased way will lead to biases in the gradient that cannot be measured easily or expressed in closed form*. This either breaks the unbiasedness assumptions made by most gradient compression results [1, 2, 3, 4] or makes error compensation over gradient biases [23, 24] difficult to adopt.

Previous efforts on activation compression [28, 29, 30, 31, 32] illustrate, albeit mostly empirically, that large deep learning models can tolerate some compression errors on these activation values. However, when it comes to the underlying theoretical analysis, these efforts mostly make assumptions that do not apply to neural networks with non-linear activation functions — the only two recent efforts that claim theoretical convergence analysis [26, 27] assume that an unbiased compression on activations leads to an unbiased error on the gradient. Not surprisingly, these algorithms lead to suboptimal quality under relatively aggressive compression, illustrated in Figure 1a — in many cases, using activation compression to fine-tune a model might be worse than zero-shot learning without any fine-tuning at all.

In this paper, we focus on the problem of activation compression for training language models over slow networks by asking the following:

- **Q1.** *Can we design an algorithm for activation compression with rigorous theoretical guarantees on SGD convergence?*
- **Q2.** *Can such an algorithm be implemented efficiently without additional runtime overhead and outperform today’s activation compression algorithms without accuracy loss?*

Our answers to both questions are **Yes**. Our Technical contributions are listed below:

**Contribution 1.** We propose AC-SGD, a novel algorithm for activation compression. The idea of AC-SGD is simple — instead of directly compressing the activations, *compress the change of activations for the same training example across epochs*. Intuitively, we expect AC-SGD to outperform simply compressing the activations because it enables an interesting “self-enforcing” dynamics: *the more training stabilizes → the smaller the changes of the model across epochs → the smaller the compression error using the same #bits → training stabilizes more*.

**Contribution 2.** The theoretical analysis of AC-SGD is non-trivial since we have to analyze the above dynamics and connect it to SGD convergence, which is quite different from most of today’s results on gradient compression and error compensation. Under mild technical conditions and quantization functions with bounded error, we show that AC-SGD converges with a rate of  $\mathcal{O}(1/\sqrt{T})$  for non-convex objectives, the same as vanilla SGD [25, 33]. To the best of our knowledge, AC-SGD is the first activation compression algorithm with rigorous theoretical analysis that shows a convergence rate of  $\mathcal{O}(1/\sqrt{T})$  (without relying on assumptions of unbiased gradient).

**Contribution 3.** We then show that AC-SGD can be optimized and implemented efficiently, without adding

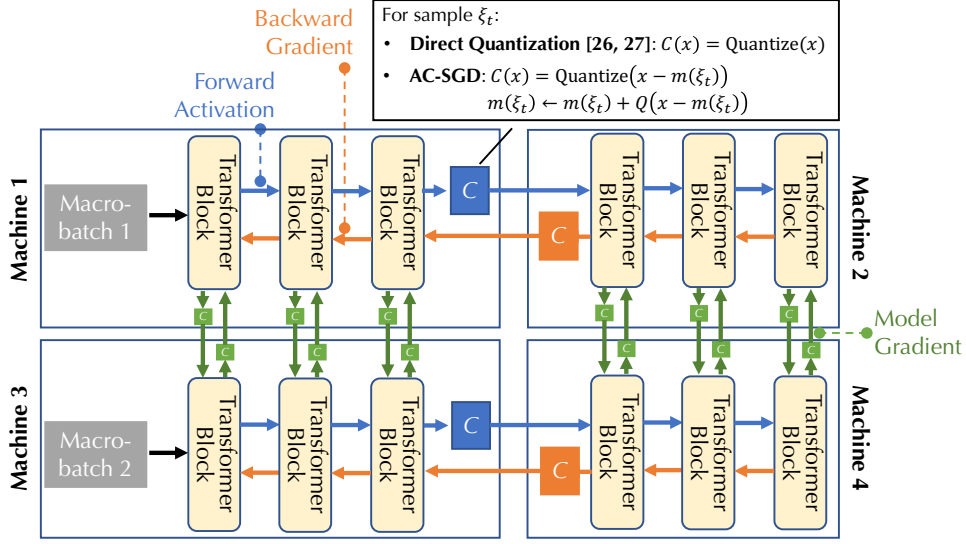


Figure 2: The communication pattern of training large language models with both data parallelism and pipeline model parallelism.  $C$  denotes a compression module. The goal of this paper is to understand the design of  $C$  for forward activation and backward gradient.

additional end-to-end runtime overhead over non-compression and other compression schemes (it does require us to utilize more memory and SSD for storage of activations).

**Contribution 4.** We then conduct extensive experiments on sequence classification and language modeling datasets using DeBERTa-1.5B and GPT2-1.5B models, respectively. We show that AC-SGD can aggressively compress activations to 2-4 bits without sacrificing convergence performance, where direct quantization of activations fails to converge; in slow networks, AC-SGD achieves up to  $4.3\times$  end-to-end speedup.

**Contribution 5.** Last but not least, we also show that AC-SGD can be combined with state-of-the-art gradient compression algorithms to enable “end-to-end communication compression”: *All data exchanges between machines, including model gradients, forward activations, and backward gradients are compressed into lower precision.* This provides up to  $4.9\times$  end-to-end speed-up, without sacrificing model quality.

## 2 Overview and Problem Formulation

Training large language models over multiple devices is a challenging task. Because of the vast number of parameters of the model and data examples, state-of-the-art systems need to combine different forms of parallelism. Figure 2 illustrates an example in which such a model is distributed over four machines: (*Pipeline Model Parallelism*) The model is partitioned onto Machine 1 and Machine 2 (similarly, Machine 3 and Machine 4), each of which is holding a subset of layers. To compute the gradient over the model using backpropagation, these two machines need to communicate the *activations* during the forward pass and the *gradient on activations* during the backward pass. (*Data Parallelism*) Machine 1 and Machine 3 (similarly, Machine 2 and Machine 4) process the same set of layers for different *macro-batches*. In this case, each of them will hold a replica of the same model. After the gradient over their model parameters are ready, they need to communicate the *model gradient*, usually by taking an average [11, 13, 14].

**Communication Compression for Forward Activations and Backward Gradients.** In slow networks, the communication among all machines often becomes the bottleneck [33]. To improve the speed of training, one can conduct *lossy compression* of the data before they are communicated, illustrated as the  $C$  module in Figure 2. When the model fits into a single machine, there have been intensive efforts on compressing the model

gradient [1, 2, 3, 4]. However, when it comes to pipeline model parallelism, such compression techniques are less studied. In this paper, we focus on designing efficient communication compression algorithms to compress both forward activations and backward gradients. As we will show later, both can be compressed significantly with AC-SGD without hurting the model quality. We also show that it is possible to combine AC-SGD with state-of-the-art gradient compression techniques to enable the end-to-end compression scheme illustrated in Figure 2.

**Problem Formulation.** In this paper, we focus on the following technical problem. Note that, for the simplicity of notations, we present here the case where the model is partitioned onto  $K = 2$  machines. AC-SGD works for cases with  $K > 2$ : (1) in experiments, we consider  $K = 8$ , i.e., a single model is partitioned onto 8 machines; (2) in the supplementary material we provide the theoretical analysis for  $K > 2$ .

Given a distribution of samples  $\mathcal{D}$ , we consider the following optimization task:

$$\min_{x \in \mathbb{R}^d} f(x) := \mathbb{E}_{\xi \sim \mathcal{D}} F(b(a(\xi, x^{(a)}), x^{(b)})), \quad (2.1)$$

where  $F$  is a loss function,  $a(-)$  and  $b(-)$  correspond to two sets of *layers* of the model —  $a(-)$  has model  $x^{(a)}$  and  $b(-)$  has model  $x^{(b)}$ . In Figure 2, Machine 1 would hold  $x^{(a)}$  and Machine 2 would hold  $x^{(b)}$ . In the following, we call the machine that holds  $x^{(a)}$  Machine  $a$  and the machine that holds  $x^{(b)}$  Machine  $b$ . In the standard backpropagation algorithm, the communication between these two machines are as follows:

- Given a data sample  $\xi$ , Machine  $a$  sends to Machine  $b$  the forward activation:  $a(\xi, x^{(a)})$
- Machine  $b$  sends to Machine  $a$  the backward gradient on  $a(\xi, x^{(a)})$ .

**Difficulties in Direct Quantization.** A natural way at compressing forward activations is to send, instead of  $a(\xi, x^{(a)})$ , a quantized version  $m(\xi, x^{(a)}) = Q(a(\xi, x^{(a)}))$ . This is the quantization scheme that state-of-the-art methods such as AC-GC [26] and TinyScript [27] use. Both AC-GC [26] and TinyScript [27] assume that gradient is unbiased when  $m(\xi, x^{(a)})$  is an unbiased estimator of  $a(\xi, x^{(a)})$ . This enables their convergence rates of  $\mathcal{O}(1/\sqrt{T})$ . However, because of the non-linearity of  $F$  and  $b$  in a deep learning model with non-linear activation functions, an unbiased  $m(\xi, x^{(a)})$  will lead to biases on the gradient. In Appendix, we will provide an example showing that such a gradient bias will hurt SGD convergence even for a very simple optimization problem. On the theory side, previous efforts on understanding gradient bias [34] also has shown that even bounded bias on gradient can impact the converges of SGD. As we will show later, empirically, this bias can indeed lead to suboptimal models under aggressive compression.

**Notation.** Throughout the paper we use the following definitions:

- $f^*$  is the optimal value of 2.1.
- $N$  is the number of samples.
- $x_t = (x_t^{(a)}, x_t^{(b)})$  is the full model at iteration  $t$ .
- $\nabla f(\cdot)$  is the gradient of function  $f$ .
- $g_{\xi_t}(x_t) = \nabla F(\xi_t; x_t)$  is the stochastic gradient.
- $Q(\cdot)$  is the quantization function used to compress activations.
- $m(\cdot)$  is the message exchanged between  $a$  and  $b$  in the feed forward path.
- $\|\cdot\|$  denotes the  $L_2$ -norm.

### 3 AC-SGD: Theoretical Analysis and System Implementations

In this section we present the AC-SGD, with the goal to mitigate the above mentioned difficulties that appear in direct quantization of the activation functions.

---

**Algorithm 1** AC-SGD Algorithm

---

```
1: Initialize:  $x_0$ , learning rate  $\gamma$ , sub-network  $a(-)$  weights  $x^{(a)}$ , sub-network  $b(-)$  weights  $x^{(b)}$ , quantization function  $Q$ , array of previous messages  $m$  initialized to 0
2: for  $t = 1, \dots, T$  do
3:   Randomly sample  $\xi_t$ 
4:   if  $\xi_t$  not seen before then
5:     Set  $m(\xi_t) = a(\xi_t, x_t^{(a)})$ 
6:   else
7:     Update  $m(\xi_t) \leftarrow m(\xi_t) + Q(a(\xi_t, x_t^{(a)}) - m(\xi_t))$ 
8:   end if
9:   // Machine  $a$  sends  $Q(a(\xi_t, x_t^{(a)}) - m(\xi_t))$  to Machine  $b$ , which knows  $m(\xi_t)$  through a local version of  $m$ 
10:  Update  $x_{t+1}^{(b)} \leftarrow x_t^{(b)} - \gamma \cdot \nabla_{x^{(b)}}(f \circ b)|_m$ 
11:  // Machine  $b$  sends  $Q(\nabla_a(f \circ b)|_m)$  to Machine  $a$ 
12:  Update  $x_{t+1}^{(a)} \leftarrow x_t^{(a)} - \gamma \cdot Q(\nabla_a(f \circ b)|_m) \cdot \nabla_{x^{(a)}} a$ 
13: end for
14: Output:  $x = (x_T^{(a)}, x_T^{(b)})$ 
```

---

### 3.1 AC-SGD Algorithm

Algorithm 1 illustrates the AC-SGD algorithm. The idea behind Algorithm 1 is simple — *instead of compressing the activations directly, compress the changes of activations for the same training example across epochs*. As illustrated in Algorithm 1, for iteration  $t$  and the data sample  $\xi_t$ , if it is the first time that  $\xi_t$  is sampled, Machine  $a$  communicates the full precision activations without any compression:  $m(\xi_t) = a(\xi_t, x_t^{(a)})$  (Lines 4-5). Both machines will save  $m(\xi_t)$  in a local buffer. If  $\xi_t$  has been sampled in previous iterations, Machine  $a$  communicates a compressed version:

$$Q(a(\xi_t, x_t^{(a)}) - m(\xi_t)),$$

where  $m(\xi_t)$  was the previous message, stored in the local buffer. Both machines then update this local buffer:

$$m(\xi_t) \leftarrow m(\xi_t) + Q(a(\xi_t, x_t^{(a)}) - m(\xi_t)).$$

Machine  $b$  then use  $m(\xi_t)$  as the forward activations, compute backward gradients, and communicate a quantized version of the backward gradient to Machine  $a$  (Line 11). We use

$$\delta_\xi = a(\xi_t, x_t^{(a)}) - m(\xi_t)$$

to denote the *message error* in sending the activations.

**Update Rules.** The above algorithm corresponds to the following update rules, at iteration  $t$  with sample  $\xi_t$ :

$$\begin{aligned} x_{t+1}^{(a)} &= x_t^{(a)} - \gamma \cdot Q(\nabla_a(f \circ b)|_{(m(\xi_t, x_t^{(a)}), x_t^{(b)})}) \cdot \nabla_{x^{(a)}} a|_{x_t^{(a)}}, \\ x_{t+1}^{(b)} &= x_t^{(b)} - \gamma \cdot \nabla_{x^{(b)}}(f \circ b)|_{(m(\xi_t, x_t^{(a)}), x_t^{(b)})}, \end{aligned}$$

where  $\gamma$  is the learning rate,  $\nabla_{x^{(b)}}(f \circ b)|_{(m(\xi_t, x_t^{(a)}), x_t^{(b)})}$  is the gradient on  $x^{(b)}$  using the compressed forward activations ( $m(\xi_t, x_t^{(a)})$ ), and  $Q(\nabla_a(f \circ b)|_{(m(\xi_t, x_t^{(a)}), x_t^{(b)})})$  is the quantized backward gradient.

Setting  $x_t = (x_t^{(a)}, x_t^{(b)})$ , we can rephrase the update rule as

$$x_{t+1} = x_t - \gamma \cdot (g_\xi(x_t) + \Delta_\xi(x_t)),$$

where  $g_\xi(x_t)$  is the stochastic gradient and  $\Delta_\xi(x_t)$  is the *gradient error* introduced by communication compression. We have  $\Delta_\xi = (\Delta_\xi^{(a)} + \Delta_\xi^{(Q)}, \Delta_\xi^{(b)})$  given by:

$$\begin{aligned} \Delta_\xi^{(Q)}(x_t) &= Q(\nabla_a(f \circ b)|_{(m(\xi_t, x_t^{(a)}), x_t^{(b)})}) \cdot \nabla_{x^{(a)}} a|_{x_t^{(a)}} - \nabla_a(f \circ b)|_{(m(\xi_t, x_t^{(a)}), x_t^{(b)})} \cdot \nabla_{x^{(a)}} a|_{x_t^{(a)}}, \\ \Delta_\xi^{(a)}(x_t) &= \nabla_a(f \circ b)|_{(m(\xi_t, x_t^{(a)}), x_t^{(b)})} \cdot \nabla_{x^{(a)}} a|_{x_t^{(a)}} - \nabla_a(f \circ b \circ a)|_{(x_t^{(a)}, x_t^{(b)})}, \\ \Delta_\xi^{(b)}(x_t) &= \nabla_{x^{(b)}}(f \circ b)|_{(m(\xi_t, x_t^{(a)}), x_t^{(b)})} - \nabla_{x^{(b)}}(f \circ b)|_{(a(\xi_t, x_t^{(a)}), x_t^{(b)})}, \end{aligned}$$

where  $\Delta_\xi^{(Q)}(x_t)$  is the error introduced by the gradient quantization in the backpropagation part, whilst  $\Delta_\xi^{(a)}(x_t)$  and  $\Delta_\xi^{(b)}(x_t)$  are the errors that the gradients of  $a$  and  $b$ , respectively, inherit from the bias introduced in the forward pass.

### 3.2 Theoretical Analysis

We now prove the main theorem which states that, under some standard assumptions that are often used in the literature [25, 33], the convergence rate of AC-SGD algorithm is  $O(1/\sqrt{T})$  for non-convex objectives, same as vanilla SGD.

**Assumptions.** We make several assumptions on the networks and the quantization. It is important to note is that we put no restrictions on either the message error  $\delta_\xi$ , nor the gradient error  $\Delta_\xi$ .

- **(A1: Lipschitz assumptions)** We assume that  $\nabla f$ ,  $\nabla(f \circ b)$  and  $a$  are  $L_f$ ,  $L_{f \circ b}$ , and  $\ell_a$ -Lipschitz, respectively, recalling that a function  $g$  is  $L_g$ -Lipschitz if

$$\|g(x) - g(y)\| \leq L_g \|x - y\|, \quad \forall x, \forall y.$$

Furthermore, we assume that  $a$  and  $f \circ b$  have gradients bounded by  $C_a$  and  $C_{f \circ b}$ , respectively, i.e.  $\|\nabla a(x)\| \leq C_a$ , and  $\|\nabla(f \circ b)(x)\| \leq C_{f \circ b}$ .

- **(A2: SGD assumptions)** We assume that the stochastic gradient  $g_\xi$  is unbiased, i.e.  $\mathbb{E}_\xi[g_\xi(x)] = \nabla f(x)$ , for all  $x$ , and with bounded variance, i.e.  $\mathbb{E}_\xi\|g_\xi(x) - \nabla f(x)\|^2 \leq \sigma^2$ , for all  $x$ .

**Theorem 3.1.** Suppose that Assumptions A1, A2 hold, and consider an unbiased quantization function  $Q(x)$  which satisfies that there exists  $c_Q < \sqrt{1/2}$  such that  $\mathbb{E}\|x - Q(x)\| \leq c_Q\|x\|$ , for all  $x$ .<sup>1</sup> Let  $\gamma = \frac{1}{3(C+3L_f)\sqrt{T}}$  be the learning rate, where

$$C = \frac{4c_Q\ell_a(1+C_a)L_{f \circ b}N}{\sqrt{1-2c_Q^2}}.$$

Then after performing  $T$  updates one has

$$\frac{1}{T} \sum_{t \in [T]} \mathbb{E}\|\nabla f(x_t)\|^2 \lesssim \frac{(C+L_f)(f(x_1) - f^*)}{\sqrt{T}} + \frac{\sigma^2 + (c_Q C_a C_{f \circ b})^2}{\sqrt{T}}. \quad (3.1)$$

We present the full proof of Theorem 3.1 in Appendix A, whereas here we explain the main intuition. The usual starting point in examining convergence rates is to use the fact that  $f$  has  $L_f$ -Lipschitz gradient. It is well known that this implies

$$\gamma \langle \nabla f(x_t), g_{\xi_t}(x_t) \rangle + f(x_{t+1}) - f(x_t) \leq -\langle \nabla f(x_t), \Delta_{\xi_t}(x_t) \rangle + \frac{\gamma^2 L_f}{2} \|g_{\xi_t}(x_t) + \Delta_{\xi_t}(x_t)\|^2.$$

After taking the expectation over all  $\xi_t$  and summing over all  $t = 1, \dots, T$ , we easily see that the key quantity to bound is  $\sum_{t=1}^T \mathbb{E}\|\tilde{\Delta}_{\xi_t}(x_t)\|^2$ , where  $\tilde{\Delta}_{\xi_t}(x_t) = (\Delta_{\xi_t}^{(a)}(x_t), \Delta_{\xi_t}^{(b)}(x_t))$ . On the other hand, the main object that we can control is the message error,  $\delta_\xi$ . Therefore, we first prove an auxiliary result which shows that  $\|\tilde{\Delta}_{\xi_t}(x_t)\| \leq (1+C_a)\ell_a\|\delta_{\xi_t}(x_t)\|$ , for all  $t$ . The key arguments for bounding  $\delta_{\xi_t}$  closely follow the self-improving loop described in the introduction, and can be summarized as follows. Since we are compressing the information in such a way that we compare with all the accumulated differences, this allows us to unwrap the changes which appeared since the last time that we observed the current sample, in an iterative way. However, since these are gradient updates, they are bounded by the learning rate — as long as we have a quantization method that keeps enough information about the signal, we can recursively build enough saving throughout the process. In particular, the more stability we have in the process, the smaller the changes of the model and the compression error gets, further strengthening the stability.

<sup>1</sup> Even for a very simple quantization function  $Q(x) = \|x\| \cdot \lceil x/\|x\| \rceil$ , where  $\lceil \cdot \rceil$  denotes rounding to the closest  $k/2^b$ , stochastically, through a simple bound  $c_Q = \sqrt{d}/2^b$ , 6 bits suffice in a low-dimensional ( $\sim 10^3$ ), 11 bits in a high-dimensional scenario ( $\sim 10^6$ ), and 16 bits in a super-high-dimensional scenario ( $\sim 10^9$ ). In practice, as we show in the experiments, we observe that for 2-4 bits are often enough for fine-tuning GPT-2 style model. This leaves interesting direction for future exploration as we expect a careful analysis of sparsity together with more advanced quantization functions can make this condition much weaker.

**Tightness.** The bound is tight with respect to quantization — setting  $c_Q = 0$  (implying  $C = 0$ ), i.e. quantization does not incur any loss, recovers the original original SGD convergence (cf. [25, 33]).

### 3.3 System Implementations and Optimizations.

**Additional storage and communication.** AC-SGD requires us to store, for each data example  $\xi$ , the compressed activation  $m(\xi)$  in a local buffer in memory or SSD. For example, in GPT2-XL training, a simple calculation shows that we need an approximately extra 1TB storage. When using data parallelism, it reduces to  $1\text{TB} / \#$  parallel degree, but also incurs communication overhead if data is shuffled in every epoch. In addition, when the example  $\xi$  is sampled again,  $m(\xi)$  needs to be (1) loaded from this local buffer to the GPU, and (2) updated when a new value for  $m(\xi)$  is ready.

**Optimization.** It is easy to implement and optimize the system such that this additional loading and updating step do not incur significant overhead on the end-to-end runtime. This is because of the fact that the GPU computation time for a forward pass is usually much longer than the data transfer time to load the activations — for GPT2-XL with 1.5 billion model parameters, a single forward pass on 6 layers require 44 ms, whereas loading  $m(\xi)$  need 0.2 ms from memory and 12 ms from SSD. One can simply pre-fetch  $m(\xi)$  right before the forward pass, and hide it within the forward pass of other data examples. Similarly, updating  $m(\xi)$  can also be hidden in the backward computation. It is also simple to reduce the communication overhead by shuffling data only once or less frequently.

## 4 Evaluation

We demonstrate that AC-SGD can significantly speed up fine-tuning large language models in slow networks. Specifically, we show: (1) on four standard benchmark tasks, AC-SGD can tolerate aggressive compression on the activations (2-4 bits) and backward gradients (4-8 bits), without hurting convergence and final loss, whereas direct quantization converges to a worse loss or even diverge, (2) in slow networks, AC-SGD provide an end-to-end speed-up up to  $4.3\times$ , and (3) AC-SGD can be combined with state-of-the-art gradient compression methods and achieve an end-to-end speed-up of up to  $4.9\times$ .

### 4.1 Experimental Setup

**Datasets and Benchmarks.** We consider both *sequence classification* and *language modeling* tasks with state-of-the-art foundation model. For the sequence classification task, we fine-tune a 1.5 billion parameter DeBERTa model<sup>2</sup> on two datasets: QNLI and CoLA. For the language modeling task, we fine-tune the GPT2 model with 1.5 billion parameters<sup>3</sup> on two datasets: WikiText2 and arXiv abstracts. All datasets are publicly available and do not contain sensitive or offensive content. Detailed setup can be found in Appendix B.

**Distributed Cluster.** We conduct our experiments on AWS with 8-32 p3.2xlarge instances, each containing a V100 GPU. For a single pipeline, we partition a model onto 8 machines. When combined with data parallelism, we use 32 instances — data parallel degree is 4 and pipeline parallel degree is 8. By default, instances are interconnected with 10Gbps bandwidth. We simulate slow networks by controlling the communication bandwidth between instances using Linux traffic control.

**Baselines.** We compare with several strong baselines:

1. FP32: in which all communications are in 32 bit floating point without any compression.
2. DirectQ [26, 27]: in which activations and backward gradients are directly compressed.

We use a simple, uniform compression scheme, which first normalizes a given vector into  $[-1, 1]$  and quantize each number into a  $b$ -bit integers by uniforming partitioning the range  $[-1, 1]$  into  $2^b$  intervals [31]. Additional details of the configuration can be found in Appendix C.

<sup>2</sup>we use the v2-xxlarge checkpoint: <https://huggingface.co/microsoft/deberta-v2-xxlarge>.

<sup>3</sup>we use the extra large checkpoint: <https://huggingface.co/gpt2-xl>.

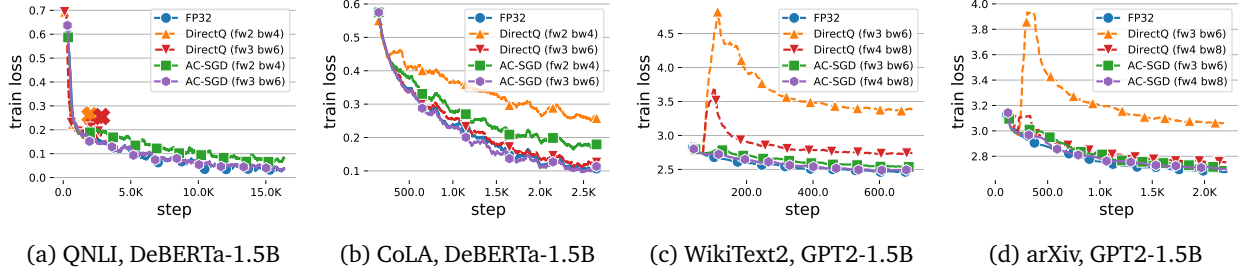


Figure 3: Convergence (loss vs. # stpes) of different approaches.  $\times$  represents divergence.

Table 2: Training Throughput. We show DeBERTa and GPT2 on QNLI and WikiText2, other tasks are similar and we leave them to Appendix.

Network Bandwidth	DeBERTa-1.5B			GPT2-1.5B		
	FP32	DirectQ fw2 bw4 / fw3 bw6	AC-SGD fw2 bw4 / fw3 bw6	FP32	DirectQ fw3 bw6 / fw4 bw8	AC-SGD fw3 bw6 / fw4 bw8
10 Gbps	$12.9 \pm 0.02$	$13.6 \pm 0.02 / 13.6 \pm 0.02$	$13.6 \pm 0.02 / 13.5 \pm 0.02$	$3.8 \pm 0.01$	$4.0 \pm 0.01 / 4.1 \pm 0.01$	$4.0 \pm 0.01 / 4.0 \pm 0.01$
1 Gbps	$9.6 \pm 0.02$	$13.3 \pm 0.02 / 13.1 \pm 0.02$	$13.3 \pm 0.02 / 13.0 \pm 0.02$	$3.2 \pm 0.01$	$4.0 \pm 0.01 / 4.0 \pm 0.01$	$4.0 \pm 0.01 / 3.9 \pm 0.01$
500 Mbps	$6.2 \pm 0.03$	$13.0 \pm 0.03 / 12.6 \pm 0.03$	$12.9 \pm 0.03 / 12.5 \pm 0.03$	$2.7 \pm 0.02$	$3.9 \pm 0.01 / 3.9 \pm 0.01$	$3.9 \pm 0.01 / 3.9 \pm 0.01$
300 Mbps	$4.4 \pm 0.04$	$12.5 \pm 0.02 / 11.9 \pm 0.03$	$12.4 \pm 0.03 / 11.8 \pm 0.03$	$1.8 \pm 0.02$	$3.9 \pm 0.01 / 3.8 \pm 0.01$	$3.8 \pm 0.01 / 3.8 \pm 0.01$
100 Mbps	$1.6 \pm 0.04$	$10.7 \pm 0.03 / 9.4 \pm 0.03$	$10.6 \pm 0.03 / 9.1 \pm 0.03$	$0.5 \pm 0.02$	$3.5 \pm 0.02 / 3.0 \pm 0.02$	$3.4 \pm 0.01 / 3.0 \pm 0.02$

**Hyperparameter Tuning.** We conduct careful tuning for all methods on all datasets. We perform grid search to choose learning rate from  $\{2.5e-6, 3e-6, 5e-6, 1e-5\}$  and macro-batch size from  $\{32, 64, 96\}$  for best model performance.

## 4.2 Results

**Convergence.** We first compare the convergence behavior of different methods. For all compression methods, we try various settings:  $fwx\ bwy$  means that we use  $x$  bits for forward activation and  $y$  bits for backward gradients. Figure 3 shows the convergence behavior for the sequence classification and language modeling tasks. FP32 converges fast since it does not introduce any compression errors. DirectQ, under aggressive compression, can converge to a significantly worse model, or even diverge. This is not surprising, given the biases on model gradients that direct quantization introduced. On the other hand, AC-SGD converges almost as fast as FP32 in terms of number of training steps.

**End-to-End Runtime.** We show the end-to-end runtime of different methods under slow networks. As illustrated in Figure 4, AC-SGD achieves a  $4.3\times$  end-to-end speed-up comparing with that of FP32 (in terms of time to the same loss), illustrating the importance of communication compression in slow networks. Table 2 shows the training throughput. Another interesting observation is that when the network is  $100\times$  slower (from 10Gbps to 100Mbps), the training is only about  $1.28\times - 1.14\times$  slower! This is exciting — if AC-SGD were to be deployed in a in real-world geo-distributed decentralized networks, the training throughput of these fine-tuning tasks would be almost as fast as the performance inside a data center!

Moreover, AC-SGD does not introduce significant runtime overhead over direct quantization. From Table 2, we see that AC-SGD is essentially as efficient as direct quantization compression in throughput.

## 4.3 End-to-end Communication Compression: AC-SGD + QuantizedAdam

AC-SGD can also be combined with existing methods on gradient compression. This allows us to compress *all* communications during training. We combine AC-SGD with QuantizedAdam [35], an error compensation-based



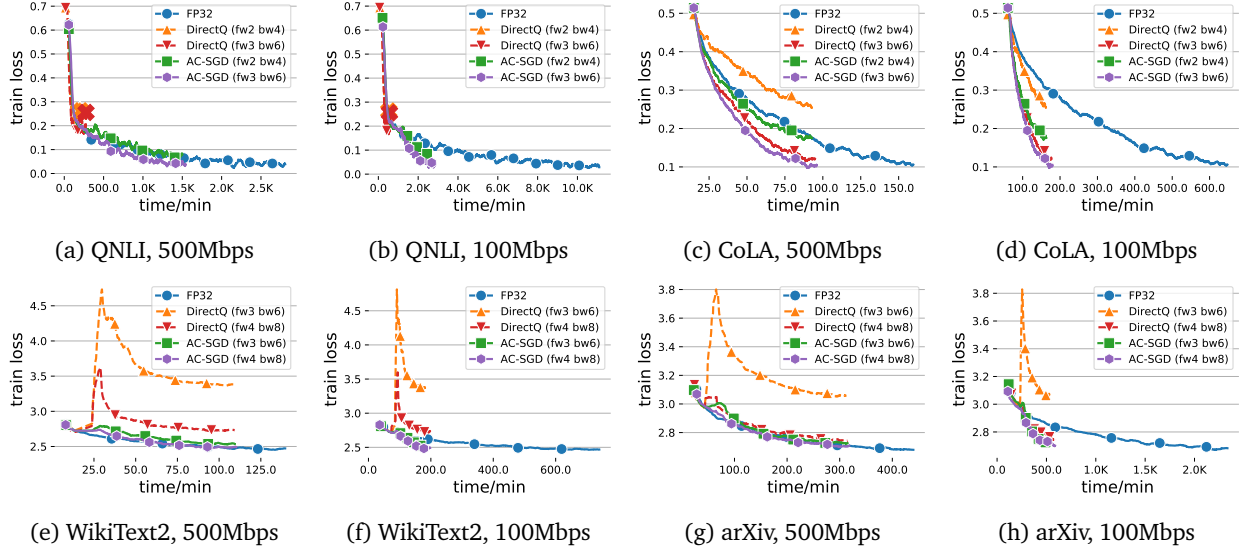


Figure 4: End-to-end training performance over different network configurations.  $\times$  represents divergence.

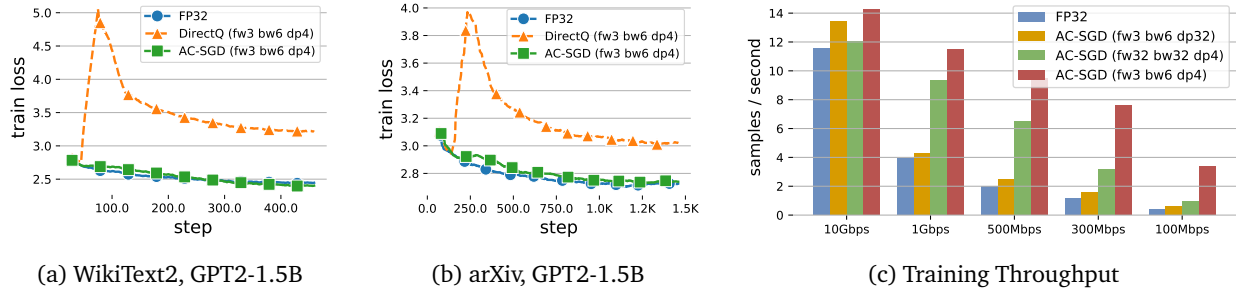


Figure 5: Convergence and Throughput of AC-SGD combined with gradient compression.

gradient compression algorithm for data parallel training.

We compress the forward activations with 3 bits, the backward gradient with 6 bits, and model gradient with 4 bits. Figure 5 illustrates the convergence and the training throughput under different network configuration. We see that AC-SGD converges well when combined with QuantizedAdam (Figure 5(a, b)). On the other hand, DirectQ, when combined with gradient compression, converges to a much worse model. In terms of training throughput, with both activation and gradient compression, we can achieve up to  $8.5\times$  throughput improvement compared to the no-compression baseline (Figure 5(c)). We also see that *both* activation and gradient compression are important in terms of improving end-to-end training throughput — as illustrated in Figure 5(c), disabling any of them will lead to a much lower training throughput.

## 5 Related Work

**Distributed training of foundation models.** Modern distributed training of deep neural networks goes beyond data parallelism [20, 36, 37, 37, 36] due to the advance of the large-scale foundation models [16], such as BERT [17], GPT-3 [18], and CLIP[19]. Popular systems to support foundation model training include Megatron [20], Deepspeed [21], and Fairscale [22]. To scale out the training of large-scale models, pipeline parallelism (e.g., Gpipe[36], Pipedream[38, 39]) is a popular option, where the model is partitioned into

multiple stages, different stages are allocated on different GPUs and the exchange of activations and gradients on activations goes through network communication.

**Communication compression of distributed learning.** Communication compression is an effective system relaxation for distributed training, especially in data parallelism [40, 41, 42, 43, 44, 45, 46, 35, 47, 48, 49, 50]. Popular techniques include quantization [1, 2, 3, 4], sparsification [51, 52, 53, 54], sketching [55, 56] and error compensation [23]. Recently, TinyScript [27] proposes to compress activations and gradients simultaneously.

**Sparse Learning for activation compression.** Sparse learning [57, 58, 59, 60, 61, 62, 63, 64, 27] has become increasingly popular for training neural networks, as it can significantly reduce the use of computation and memory while preserving the generalization of such models. In particular, activation compression methods [28, 29, 30, 31, 32, 26] are proposed to reduce the memory footprint by adopting lossless [65, 66, 67] and lossy [68, 26, 69] compression techniques in the training of various deep neural networks (e.g., CNN[61, 70, 71], GNN[72]). These approaches usually compute the activation with *full precision* in forward propagation, adopt the compression method over the activation, and store the compressed version in DRAM for later use in backward propagation. Thus, compression does not introduce any error in forward propagation in contrast to the scenario of communicating compressed activation in the distributed setting.

**Delta-based compression.** Delta-based compression [73] is a classic solution to various system problems. Recent research has also used the property of spatial proximity within activation in neural network training based on empirical observations [74, 75, 69]. However, to our knowledge, no attempt has been made to consider the proximity of activation through training epochs to enable efficient compression with theoretical guarantee.

## 6 Conclusion

In this paper, we discuss how to adopt communication compression for activations in distributed learning. We proposed AC-SGD, a novel activation compression algorithm for communication-efficient pipeline parallelism training over slow networks. AC-SGD achieves  $O(1/\sqrt{T})$  convergence rate for non-convex optimization without making assumptions on gradient unbiasedness. Our empirical study suggests that AC-SGD can achieve up to  $4.3\times$  speedup for pipeline parallelism. When combined with gradient compression in data parallelism, the end-to-end speed-up can be up to  $4.9\times$ .

## References

- [1] Dan Alistarh, Demjan Grubic, Jerry Li, Ryota Tomioka, and Milan Vojnovic. Qsgd: Communication-efficient sgd via gradient quantization and encoding. *arXiv preprint arXiv:1610.02132*, 2016.
- [2] Hantian Zhang, Jerry Li, Kaan Kara, Dan Alistarh, Ji Liu, and Ce Zhang. Zipml: Training linear models with end-to-end low precision, and a little bit of deep learning. In *International Conference on Machine Learning*, pages 4035–4043. PMLR, 2017.
- [3] Jeremy Bernstein, Yu-Xiang Wang, Kamyar Azizzadenesheli, and Animashree Anandkumar. signsgd: Compressed optimisation for non-convex problems. In *International Conference on Machine Learning*, pages 560–569. PMLR, 2018.
- [4] Wei Wen, Cong Xu, Feng Yan, Chunpeng Wu, Yandan Wang, Yiran Chen, and Hai Li. Terngrad: ternary gradients to reduce communication in distributed deep learning. In *Proceedings of the 31st International Conference on Neural Information Processing Systems*, pages 1508–1518, 2017.
- [5] Anastasia Koloskova, Sebastian Stich, and Martin Jaggi. Decentralized stochastic optimization and gossip algorithms with compressed communication. In *International Conference on Machine Learning*, pages 3478–3487. PMLR, 2019.

- [6] Youjie Li, Mingchao Yu, Songze Li, Salman Avestimehr, Nam Sung Kim, and Alexander Schwing. Pipe-sgd: a decentralized pipelined sgD framework for distributed deep net training. In *Proceedings of the 32nd International Conference on Neural Information Processing Systems*, pages 8056–8067, 2018.
- [7] Xiangru Lian, Ce Zhang, Huan Zhang, Cho-Jui Hsieh, Wei Zhang, and Ji Liu. Can decentralized algorithms outperform centralized algorithms? a case study for decentralized parallel stochastic gradient descent. In *Proceedings of the 31st International Conference on Neural Information Processing Systems*, pages 5336–5346, 2017.
- [8] Xiangru Lian, Wei Zhang, Ce Zhang, and Ji Liu. Asynchronous decentralized parallel stochastic gradient descent. In *International Conference on Machine Learning*, pages 3043–3052. PMLR, 2018.
- [9] Hanlin Tang, Shaoduo Gan, Ce Zhang, Tong Zhang, and Ji Liu. Communication compression for decentralized training. In *Proceedings of the 32nd International Conference on Neural Information Processing Systems*, pages 7663–7673, 2018.
- [10] Hanlin Tang, Xiangru Lian, Ming Yan, Ce Zhang, and Ji Liu. D2: Decentralized training over decentralized data. In *International Conference on Machine Learning*, pages 4848–4856. PMLR, 2018.
- [11] Shen Li, Yanli Zhao, Rohan Varma, Omkar Salpekar, Pieter Noordhuis, Teng Li, Adam Paszke, Jeff Smith, Brian Vaughan, Pritam Damania, et al. Pytorch distributed: Experiences on accelerating data parallel training. *Proceedings of the VLDB Endowment*, 13(12).
- [12] Pytorch-lightning. <https://www.pytorchlightning.ai/>.
- [13] Alexander Sergeev and Mike Del Balso. Horovod: fast and easy distributed deep learning in tensorflow. *arXiv preprint arXiv:1802.05799*, 2018.
- [14] Gan, Shaoduo and Lian, Xiangru and Wang, Rui and Chang, Jianbin and Liu, Chengjun and Shi, Hongmei and Zhang, Shengzhuo and Li, Xianghong and Sun, Tengxu and Jiang, Jiawei and others. BAGUA: scaling up distributed learning with system relaxations. *Proceedings of the VLDB Endowment*, 15(4):804–813, 2021.
- [15] Yimin Jiang, Yibo Zhu, Chang Lan, Bairen Yi, Yong Cui, and Chuanxiong Guo. A unified architecture for accelerating distributed {DNN} training in heterogeneous gpu/cpu clusters. In *14th {USENIX} Symposium on Operating Systems Design and Implementation ({OSDI} 20)*, pages 463–479, 2020.
- [16] Rishi Bommasani, Drew A. Hudson, Ehsan Adeli, Russ Altman, Simran Arora, Sydney von Arx, Michael S. Bernstein, Jeannette Bohg, Antoine Bosselut, Emma Brunskill, Erik Brynjolfsson, Shyamal Buch, Dallas Card, Rodrigo Castellon, Niladri S. Chatterji, Annie S. Chen, Kathleen Creel, Jared Quincy Davis, Dorottya Demszky, Chris Donahue, Moussa Doumbouya, Esin Durmus, Stefano Ermon, John Etchemendy, Kawin Ethayarajh, Li Fei-Fei, Chelsea Finn, Trevor Gale, Lauren Gillespie, Karan Goel, Noah D. Goodman, Shelby Grossman, Neel Guha, Tatsunori Hashimoto, Peter Henderson, John Hewitt, Daniel E. Ho, Jenny Hong, Kyle Hsu, Jing Huang, Thomas Icard, Saahil Jain, Dan Jurafsky, Pratyusha Kalluri, Siddharth Karamcheti, Geoff Keeling, Fereshte Khani, Omar Khattab, Pang Wei Koh, Mark S. Krass, Ranjay Krishna, Rohith Kuditipudi, and et al. On the opportunities and risks of foundation models. *CoRR*, abs/2108.07258, 2021.
- [17] Jacob Devlin, Ming-Wei Chang, Kenton Lee, and Kristina Toutanova. Bert: Pre-training of deep bidirectional transformers for language understanding. *arXiv preprint arXiv:1810.04805*, 2018.
- [18] Tom Brown, Benjamin Mann, Nick Ryder, Melanie Subbiah, Jared D Kaplan, Prafulla Dhariwal, Arvind Neelakantan, Pranav Shyam, Girish Sastry, Amanda Askell, et al. Language models are few-shot learners. *Advances in neural information processing systems*, 33:1877–1901, 2020.
- [19] Alec Radford, Jong Wook Kim, Chris Hallacy, Aditya Ramesh, Gabriel Goh, Sandhini Agarwal, Girish Sastry, Amanda Askell, Pamela Mishkin, Jack Clark, et al. Learning transferable visual models from natural language supervision. In *International Conference on Machine Learning*, pages 8748–8763. PMLR, 2021.

- [20] Mohammad Shoeybi, Mostofa Patwary, Raul Puri, Patrick LeGresley, Jared Casper, and Bryan Catanzaro. Megatron-lm: Training multi-billion parameter language models using model parallelism. *arXiv preprint arXiv:1909.08053*, 2019.
- [21] Jeff Rasley, Samyam Rajbhandari, Olatunji Ruwase, and Yuxiong He. Deepspeed: System optimizations enable training deep learning models with over 100 billion parameters. In *Proceedings of the 26th ACM SIGKDD International Conference on Knowledge Discovery & Data Mining*, pages 3505–3506, 2020.
- [22] Mandeep Baines, Shruti Bhosale, Vittorio Caggiano, Naman Goyal, Siddharth Goyal, Myle Ott, Benjamin Lefaudeux, Vitaliy Liptchinsky, Mike Rabbat, Sam Sheiffer, et al. FairScale: A general purpose modular pytorch library for high performance and large scale training, 2021.
- [23] Hanlin Tang, Chen Yu, Xiangru Lian, Tong Zhang, and Ji Liu. Doublesqueeze: Parallel stochastic gradient descent with double-pass error-compensated compression. In *International Conference on Machine Learning*, pages 6155–6165. PMLR, 2019.
- [24] Hanlin Tang, Xiangru Lian, Shuang Qiu, Lei Yuan, Ce Zhang, Tong Zhang, and Ji Liu. Deepsqueeze: Parallel stochastic gradient descent with double-pass error-compensated compression. *arXiv preprint arXiv:1907.07346*, 2019.
- [25] Léon Bottou, Frank E Curtis, and Jorge Nocedal. Optimization methods for large-scale machine learning. *Siam Review*, 60(2):223–311, 2018.
- [26] R David Evans and Tor Aamodt. Ac-gc: Lossy activation compression with guaranteed convergence. *Advances in Neural Information Processing Systems*, 34, 2021.
- [27] Fangcheng Fu, Yuzheng Hu, Yihan He, Jiawei Jiang, Yingxia Shao, Ce Zhang, and Bin Cui. Don’t waste your bits! squeeze activations and gradients for deep neural networks via tinscript. In *International Conference on Machine Learning*, pages 3304–3314. PMLR, 2020.
- [28] Song Han, Huizi Mao, and William J Dally. Deep compression: Compressing deep neural networks with pruning, trained quantization and huffman coding. 2016.
- [29] Itay Hubara, Matthieu Courbariaux, Daniel Soudry, Ran El-Yaniv, and Yoshua Bengio. Quantized neural networks: Training neural networks with low precision weights and activations. *The Journal of Machine Learning Research*, 18(1):6869–6898, 2017.
- [30] Animesh Jain, Amar Phanishayee, Jason Mars, Lingjia Tang, and Gennady Pekhimenko. Gist: Efficient data encoding for deep neural network training. In *2018 ACM/IEEE 45th Annual International Symposium on Computer Architecture (ISCA)*, pages 776–789. IEEE, 2018.
- [31] Ayan Chakrabarti and Benjamin Moseley. Backprop with approximate activations for memory-efficient network training. *Advances in Neural Information Processing Systems*, 32, 2019.
- [32] Jianfei Chen, Lianmin Zheng, Zhewei Yao, Dequan Wang, Ion Stoica, Michael Mahoney, and Joseph Gonzalez. Actnn: Reducing training memory footprint via 2-bit activation compressed training. In *International Conference on Machine Learning*, pages 1803–1813. PMLR, 2021.
- [33] Ji Liu and Ce Zhang. Distributed learning systems with first-order methods. *arXiv preprint arXiv:2104.05245*, 2021.
- [34] Ahmad Ajalloeian and Sebastian U. Stich. On the convergence of sgd with biased gradients, 2020.
- [35] Hanlin Tang, Shaoduo Gan, Ammar Ahmad Awan, Samyam Rajbhandari, Conglong Li, Xiangru Lian, Ji Liu, Ce Zhang, and Yuxiong He. 1-bit adam: Communication efficient large-scale training with adam’s convergence speed. In *International Conference on Machine Learning*, pages 10118–10129. PMLR, 2021.

- [36] Yanping Huang, Youlong Cheng, Ankur Bapna, Orhan Firat, Dehao Chen, Mia Chen, Hyoungho Lee, Jiquan Ngiam, Quoc V Le, Yonghui Wu, et al. Gpipe: Efficient training of giant neural networks using pipeline parallelism. *Advances in neural information processing systems*, 32, 2019.
- [37] Bowen Yang, Jian Zhang, Jonathan Li, Christopher Ré, Christopher Aberger, and Christopher De Sa. Pipemare: Asynchronous pipeline parallel dnn training. *Proceedings of Machine Learning and Systems*, 3:269–296, 2021.
- [38] Deepak Narayanan, Aaron Harlap, Amar Phanishayee, Vivek Seshadri, Nikhil R Devanur, Gregory R Ganger, Phillip B Gibbons, and Matei Zaharia. Pipedream: generalized pipeline parallelism for dnn training. In *Proceedings of the 27th ACM Symposium on Operating Systems Principles*, pages 1–15, 2019.
- [39] Deepak Narayanan, Amar Phanishayee, Kaiyu Shi, Xie Chen, and Matei Zaharia. Memory-efficient pipeline-parallel dnn training. In *International Conference on Machine Learning*, pages 7937–7947. PMLR, 2021.
- [40] Chia-Yu Chen, Jiamin Ni, Songtao Lu, Xiaodong Cui, Pin-Yu Chen, Xiao Sun, Naigang Wang, Swagath Venkataramani, Vijayalakshmi Viji Srinivasan, Wei Zhang, et al. Scalecom: Scalable sparsified gradient compression for communication-efficient distributed training. *Advances in Neural Information Processing Systems*, 33:13551–13563, 2020.
- [41] Cong Xie, Shuai Zheng, Sanmi Koyejo, Indranil Gupta, Mu Li, and Haibin Lin. Cser: Communication-efficient sgd with error reset. *Advances in Neural Information Processing Systems*, 33:12593–12603, 2020.
- [42] Fartash Faghri, Iman Tabrizian, Ilia Markov, Dan Alistarh, Daniel M Roy, and Ali Ramezani-Kebrya. Adaptive gradient quantization for data-parallel sgd. *Advances in neural information processing systems*, 33:3174–3185, 2020.
- [43] Zhize Li, Dmitry Kovalev, Xun Qian, and Peter Richtárik. Acceleration for compressed gradient descent in distributed and federated optimization. In *International Conference on Machine Learning*, pages 5895–5904. PMLR, 2020.
- [44] Daniel Rothchild, Ashwinee Panda, Enayat Ullah, Nikita Ivkin, Ion Stoica, Vladimir Braverman, Joseph Gonzalez, and Raman Arora. Fetchsgd: Communication-efficient federated learning with sketching. In *International Conference on Machine Learning*, pages 8253–8265. PMLR, 2020.
- [45] Mher Safaryan and Peter Richtárik. Stochastic sign descent methods: New algorithms and better theory. In *International Conference on Machine Learning*, pages 9224–9234. PMLR, 2021.
- [46] Eduard Gorbunov, Konstantin P Burlachenko, Zhize Li, and Peter Richtárik. Marina: Faster non-convex distributed learning with compression. In *International Conference on Machine Learning*, pages 3788–3798. PMLR, 2021.
- [47] Mher Safaryan, Filip Hanzely, and Peter Richtárik. Smoothness matrices beat smoothness constants: better communication compression techniques for distributed optimization. *Advances in Neural Information Processing Systems*, 34, 2021.
- [48] Xun Qian, Peter Richtárik, and Tong Zhang. Error compensated distributed sgd can be accelerated. *Advances in Neural Information Processing Systems*, 34, 2021.
- [49] Ahmed M Abdelmoniem, Ahmed Elzanaty, Mohamed-Slim Alouini, and Marco Canini. An efficient statistical-based gradient compression technique for distributed training systems. *Proceedings of Machine Learning and Systems*, 3:297–322, 2021.
- [50] Hongyi Wang, Saurabh Agarwal, and Dimitris Papailiopoulos. Pufferfish: Communication-efficient models at no extra cost. *Proceedings of Machine Learning and Systems*, 3:365–386, 2021.

- [51] J Wangni, J Liu, J Wang, and T Zhang. Gradient sparsification for communication-efficient distributed optimization. *Advances in Neural Information Processing Systems*, 31:1299, 2018.
- [52] Dan Alistarh, Torsten Hoefer, Mikael Johansson, Sarit Khirirat, Nikola Konstantinov, and Cédric Renggli. The convergence of sparsified gradient methods. In *Proceedings of the 32nd International Conference on Neural Information Processing Systems*, pages 5977–5987, 2018.
- [53] Hongyi Wang, Scott Sievert, Zachary Charles, Shengchao Liu, Stephen Wright, and Dimitris Papailiopoulos. Atomo: communication-efficient learning via atomic sparsification. In *Proceedings of the 32nd International Conference on Neural Information Processing Systems*, pages 9872–9883, 2018.
- [54] Jialei Wang, Mladen Kolar, Nathan Srebro, and Tong Zhang. Efficient distributed learning with sparsity. In *International Conference on Machine Learning*, pages 3636–3645. PMLR, 2017.
- [55] Jiawei Jiang, Fangcheng Fu, Tong Yang, and Bin Cui. Sketchml: Accelerating distributed machine learning with data sketches. In *Proceedings of the 2018 ACM SIGMOD International Conference on Management of Data*, pages 1269–1284, 2018.
- [56] Nikita Ivkin, Daniel Rothchild, Enayat Ullah, Ion Stoica, Raman Arora, et al. Communication-efficient distributed sgd with sketching. In *Advances in Neural Information Processing Systems*, pages 13144–13154, 2019.
- [57] Decebal Constantin Mocanu, Elena Mocanu, Peter Stone, Phuong H Nguyen, Madeleine Gibescu, and Antonio Liotta. Scalable training of artificial neural networks with adaptive sparse connectivity inspired by network science. *Nature communications*, 9(1):1–12, 2018.
- [58] Md Aamir Raihan and Tor Aamodt. Sparse weight activation training. *Advances in Neural Information Processing Systems*, 33:15625–15638, 2020.
- [59] Beidi Chen, Tri Dao, Kaizhao Liang, Jiaming Yang, Zhao Song, Atri Rudra, and Christopher Re. Pixelated butterfly: Simple and efficient sparse training for neural network models. *arXiv preprint arXiv:2112.00029*, 2021.
- [60] Tim Dettmers and Luke Zettlemoyer. Sparse networks from scratch: Faster training without losing performance. *arXiv preprint arXiv:1907.04840*, 2019.
- [61] Hesham Mostafa and Xin Wang. Parameter efficient training of deep convolutional neural networks by dynamic sparse reparameterization. In *International Conference on Machine Learning*, pages 4646–4655. PMLR, 2019.
- [62] LIU Junjie, XU Zhe, SHI Runbin, Ray CC Cheung, and Hayden KH So. Dynamic sparse training: Find efficient sparse network from scratch with trainable masked layers. In *International Conference on Learning Representations*, 2019.
- [63] Torsten Hoefer, Dan Alistarh, Tal Ben-Nun, Nikoli Dryden, and Alexandra Peste. Sparsity in deep learning: Pruning and growth for efficient inference and training in neural networks. *Journal of Machine Learning Research*, 22(241):1–124, 2021.
- [64] Shiwei Liu, Tianlong Chen, Xiaohan Chen, Zahra Atashgahi, Lu Yin, Huanyu Kou, Li Shen, Mykola Pechenizkiy, Zhangyang Wang, and Decebal Constantin Mocanu. Sparse training via boosting pruning plasticity with neuroregeneration. *Advances in Neural Information Processing Systems*, 34, 2021.
- [65] Esha Choukse, Michael B Sullivan, Mike O’Connor, Mattan Erez, Jeff Pool, David Nellans, and Stephen W Keckler. Buddy compression: Enabling larger memory for deep learning and hpc workloads on gpus. In *2020 ACM/IEEE 47th Annual International Symposium on Computer Architecture (ISCA)*, pages 926–939. IEEE, 2020.

- [66] Minsoo Rhu, Mike O'Connor, Niladrish Chatterjee, Jeff Pool, Youngeun Kwon, and Stephen W Keckler. Compressing dma engine: Leveraging activation sparsity for training deep neural networks. In *2018 IEEE International Symposium on High Performance Computer Architecture (HPCA)*, pages 78–91. IEEE, 2018.
- [67] Alberto Delmás Lascorz, Sayeh Sharify, Isak Edo, Dylan Malone Stuart, Omar Mohamed Awad, Patrick Judd, Mostafa Mahmoud, Milos Nikolic, Kevin Siu, Zissis Poulos, et al. Shapeshifter: Enabling fine-grain data width adaptation in deep learning. In *Proceedings of the 52nd Annual IEEE/ACM International Symposium on Microarchitecture*, pages 28–41, 2019.
- [68] Sian Jin, Guanpeng Li, Shuaiwen Leon Song, and Dingwen Tao. A novel memory-efficient deep learning training framework via error-bounded lossy compression. In *Proceedings of the 26th ACM SIGPLAN Symposium on Principles and Practice of Parallel Programming*, pages 485–487, 2021.
- [69] R David Evans, Lufei Liu, and Tor M Aamodt. Jpeg-act: accelerating deep learning via transform-based lossy compression. In *2020 ACM/IEEE 47th Annual International Symposium on Computer Architecture (ISCA)*, pages 860–873. IEEE, 2020.
- [70] Georgios Georgiadis. Accelerating convolutional neural networks via activation map compression. In *Proceedings of the IEEE/CVF Conference on Computer Vision and Pattern Recognition*, pages 7085–7095, 2019.
- [71] Denis Gudovskiy, Alec Hodgkinson, and Luca Rigazio. Dnn feature map compression using learned representation over gf (2). In *Proceedings of the European Conference on Computer Vision (ECCV) Workshops*, pages 0–0, 2018.
- [72] Zirui Liu, Kaixiong Zhou, Fan Yang, Li Li, Rui Chen, and Xia Hu. Exact: Scalable graph neural networks training via extreme activation compression. In *International Conference on Learning Representations*, 2021.
- [73] Gennady Pekhimenko, Vivek Seshadri, Onur Mutlu, Michael A Kozuch, Phillip B Gibbons, and Todd C Mowry. Base-delta-immediate compression: Practical data compression for on-chip caches. In *2012 21st international conference on parallel architectures and compilation techniques (PACT)*, pages 377–388. IEEE, 2012.
- [74] Omar Mohamed Awad, Mostafa Mahmoud, Isak Edo, Ali Hadi Zadeh, Ciaran Bannon, Anand Jayarajan, Gennady Pekhimenko, and Andreas Moshovos. Fpraker: A processing element for accelerating neural network training. In *MICRO-54: 54th Annual IEEE/ACM International Symposium on Microarchitecture*, pages 857–869, 2021.
- [75] Andrei Bersatti, Nima Shoghi Ghalehshahi, and Hyesoon Kim. Neural network weight compression with nnw-bdi. In *The International Symposium on Memory Systems*, pages 335–340, 2020.

## A Proof of the Main Theorem

In this section we prove Theorem 3.1. The main idea comes from the “self-enforcing” dynamics described in the introduction of this work: *the more training stabilizes  $\rightarrow$  the smaller the changes of the model across epochs  $\rightarrow$  the smaller the changes of activations for the same training example across epochs  $\rightarrow$  the smaller the compression error using the same #bits  $\rightarrow$  training stabilizes more.*

We start by providing two auxiliary results. The first one connects the message error and the gradient error.

**Lemma A.1.** *For every sample  $\xi$ , one has*

$$\|\Delta_\xi^{(Q)}(x)\| \leq c_Q C_a C_{f \circ b},$$

and

$$\|\tilde{\Delta}_\xi(x)\| \leq (1 + C_a) L_{f \circ b} \|\delta_\xi(x)\|,$$

where  $\tilde{\Delta}_\xi(x) = (\Delta_\xi^{(a)}(x), \Delta_\xi^{(b)})$ .

**PROOF:** Note that

$$\begin{aligned} \|\Delta_\xi^{(Q)}(x_t)\| &= \|\nabla_x a(\xi, x)_{x=x_t^{(a)}}\| \cdot \|Q(\nabla_x(f \circ b)(x, x_t^{(b)})_{x=m(\xi, x_t^{(a)})} - \nabla_x(f \circ b)(x, x_t^{(b)})_{x=m(\xi, x_t^{(a)})})\| \\ &\leq C_a c_Q \|\nabla_x(f \circ b)(x, x_t^{(b)})_{x=m(\xi, x_t^{(a)})}\| \leq c_Q C_a C_{f \circ b}, \\ \|\Delta_\xi^{(a)}(x_t)\| &= \|\nabla_x a(\xi, x)_{x=x_t^{(a)}}\| \cdot \|\nabla_x(f \circ b)(x, x_t^{(b)})_{x=m(\xi, x_t^{(a)})} - \nabla_x(f \circ b)(x, x_t^{(b)})_{x=a(\xi, x_t^{(a)})}\| \\ &\leq C_a L_{f \circ b} \|(m(\xi, x_t^{(a)}), x_t^{(b)}) - (a(\xi, x_t^{(a)}), x_t^{(b)})\| = C_a L_{f \circ b} \|\delta_\xi(x_t)\|, \\ \|\Delta_\xi^{(b)}(x_t)\| &= \|\nabla_y(f \circ b)(m(\xi, x_t^{(a)}), y)_{y=x_t^{(b)}} - \nabla_y(f \circ b)(a(\xi, x_t^{(a)}), y)_{y=x_t^{(b)}}\| \\ &\leq L_{f \circ b} \|(m(\xi, x_t^{(a)}), x_t^{(b)}) - (a(\xi, x_t^{(a)}), x_t^{(b)})\| = L_{f \circ b} \|\delta_\xi(x_t)\|, \end{aligned}$$

which together with  $\|\tilde{\Delta}_\xi(x_t)\| = \|\Delta_\xi^{(a)}(x_t)\| + \|\Delta_\xi^{(b)}(x_t)\|$  yields the claim.  $\blacksquare$

We now prove that the message error can be efficiently bounded by the true gradient.

**Lemma A.2.** *For  $C' = \frac{18c_Q^2 L_a^2 N^2}{1 - 2c_Q^2}$ , one has*

$$\frac{1}{T} \sum_{t \in [T]} \mathbb{E} \|\delta_{\xi_t}(x_t)\|^2 \leq C' \gamma^2 \cdot \left( \frac{1}{T} \sum_{t \in [T]} \mathbb{E} \|\nabla f(x_t)\|^2 + \sigma^2 + (c_Q C_a C_{f \circ b})^2 \right).$$

**PROOF:** Let  $\xi$  be a fixed sample. To simplify the exposition, we abuse the notation slightly by  $a(x) = a(\xi, x)$ ,  $m(x) = m(\xi, x)$ . Let  $T(\xi)$  be the number of realizations of  $\xi$  before time  $T$ . Using the definition of  $\delta_\xi$  (recalling that  $\delta_\xi(x_{t_1(\xi)}) = 0$ , since in the first iteration we send the correct signal), we have

$$\begin{aligned} \sum_{k=1}^{T(\xi)} \|\delta_\xi(x_{t_k(\xi)})\|^2 &= \sum_{k=2}^{T(\xi)} \|a(x_{t_k(\xi)}) - m(x_{t_k(\xi)})\|^2 \\ &= \sum_{k=2}^{T(\xi)} \|a(x_{t_k(\xi)}) - m(x_{t_{k-1}(\xi)}) - Q(a(x_{t_k(\xi)}) - m(x_{t_{k-1}(\xi)}))\|^2 \\ \{\|x - Q(x)\| \leq c_Q \|x\|\} &\leq c_Q^2 \sum_{k=2}^{T(\xi)} \|a(x_{t_k(\xi)}) - a(x_{t_{k-1}(\xi)}) + \delta_\xi(x_{t_{k-1}(\xi)})\|^2 \\ \{(\alpha + \beta)^2 \leq 2\alpha^2 + 2\beta^2\} &\leq 2c_Q^2 \sum_{k=2}^{T(\xi)} \|a(x_{t_k(\xi)}) - a(x_{t_{k-1}(\xi)})\|^2 + 2c_Q^2 \sum_{k=2}^{T(\xi)} \|\delta_\xi(x_{t_{k-1}(\xi)})\|^2 \\ \{a \text{ is } \ell_a\text{-Lipschitz}\} &\leq 2c_Q^2 \ell_a^2 \sum_{k=2}^{T(\xi)} \|x_{t_k(\xi)} - x_{t_{k-1}(\xi)}\|^2 + 2c_Q^2 \sum_{k=2}^{T(\xi)} \|\delta_\xi(x_{t_{k-1}(\xi)})\|^2. \end{aligned}$$



Transferring the  $\delta_\xi$  part to the LHS, and noting that between every two realizations of  $\xi$  at times  $t_{k-1}(\xi)$  and  $t_k(\xi)$ , we can follow updates for  $t = t_{k-1}(\xi), \dots, t_k(\xi) - 1$ , we get

$$\begin{aligned} (1-2c_Q^2) \sum_{k=1}^{T(\xi)} \|\delta_\xi(x_{t_k(\xi)})\|^2 &\leq \gamma^2 \cdot (2c_Q^2 \ell_a^2) \sum_{k=1}^{T(\xi)} \left\| \sum_{t=t_{k-1}(\xi)}^{t_k(\xi)-1} (g_{\xi_t}(x_t) + \Delta_{\xi_t}(x_t)) \right\|^2 \\ \{\text{Cauchy-Schwarz}\} &\leq \gamma^2 \cdot (2c_Q^2 \ell_a^2) \sum_{k=1}^{T(\xi)} (t_k(\xi) - t_{k-1}(\xi)) \sum_{t=t_{k-1}(\xi)}^{t_k(\xi)-1} \|g_{\xi_t}(x_t) + \Delta_{\xi_t}(x_t)\|^2 \\ &= \gamma^2 \cdot (2c_Q^2 \ell_a^2) \sum_{t \in [T]} \omega_\xi(t) \cdot \|g_{\xi_t}(x_t) + \Delta_{\xi_t}(x_t)\|^2, \end{aligned}$$

where  $\omega: [T] \rightarrow \{0, 1, \dots\}$  is defined by  $\omega_\xi(t) = t_k(\xi) - t_{k-1}(\xi)$ , if  $t \in [t_{k-1}(\xi), t_k(\xi) - 1]$ , and  $\omega_\xi(t) = 0$ , if  $t > t_{T(\xi)}(\xi)$ . We note that for two different samples  $\xi$  and  $\xi'$ , the sums on the LHS are disjoint. Therefore, summing over all samples  $\xi$  and taking the expectation over  $\xi$  and all  $\xi_t$  yields

$$\begin{aligned} (1-2c_Q^2) \cdot \frac{1}{T} \sum_{t \in [T]} \mathbb{E} \|\delta_{\xi_t}(x_t)\|^2 &\leq \gamma^2 \cdot (2c_Q^2 \ell_a^2) \cdot \frac{1}{T} \sum_{t \in [T]} \mathbb{E} \|g_{\xi_t}(x_t) + \Delta_{\xi_t}(x_t)\|^2 \cdot N \cdot \mathbb{E}[\omega_\xi(t)] \\ &\leq \gamma^2 \cdot (2c_Q^2 \ell_a^2 N^2) \cdot \frac{1}{T} \sum_{t \in [T]} \mathbb{E} \|g_{\xi_t}(x_t) + \Delta_{\xi_t}(x_t)\|^2, \end{aligned}$$

since  $\mathbb{E}[\omega_\xi(t)] \leq N$ . Applying  $\|g_{\xi_t}(x_t) + \Delta_{\xi_t}(x_t)\|^2 \leq 3\|g_{\xi_t}(x_t)\|^2 + 3\|\Delta_{\xi_t}^{(Q)}(x_t)\|^2 + 3\|\tilde{\Delta}_{\xi_t}(x_t)\|^2$ , bounded variance  $\mathbb{E}\|g_\xi(x) - \nabla f(x)\|^2 \leq \sigma^2$ , and Lemma A.1, we get

$$\begin{aligned} (1-2c_Q^2 - \gamma^2 \cdot 6c_Q^2 \ell_a^2 N^2 (1+C_a)^2 L_{fob}^2) \cdot \frac{1}{T} \sum_{t \in [T]} \mathbb{E} \|\delta_{\xi_t}(x_t)\|^2 \\ \leq \gamma^2 \cdot (6c_Q^2 \ell_a^2 N^2) \left( 2\sigma^2 + 2 \cdot \frac{1}{T} \sum_{t \in [T]} \mathbb{E} \|\nabla f(x_t)\|^2 + (c_Q C_a C_{fob})^2 \right), \end{aligned}$$

which implies

$$\begin{aligned} \left( 1 - 2c_Q^2 - \gamma^2 \cdot \frac{3}{8} \cdot C^2 \cdot (1-2c_Q^2) \right) \cdot \frac{1}{T} \sum_{t \in [T]} \mathbb{E} \|\delta_{\xi_t}(x_t)\|^2 \\ \leq \gamma^2 \cdot (12c_Q^2 \ell_a^2 N^2) \left( \sigma^2 + \frac{1}{T} \sum_{t \in [T]} \mathbb{E} \|\nabla f(x_t)\|^2 + (c_Q C_a C_{fob})^2 \right), \end{aligned}$$

Recalling the definitions of  $C$  and  $\gamma$ , and the fact that  $\gamma \cdot C < \frac{1}{3}$ , we can simplify the LHS to get

$$(1-2c_Q^2) \cdot \frac{1}{T} \sum_{t \in [T]} \mathbb{E} \|\delta_{\xi_t}(x_t)\|^2 \leq \gamma^2 \cdot (12 \cdot \frac{24}{23} \cdot c_Q^2 \ell_a^2 N^2) \left( \sigma^2 + \frac{1}{T} \sum_{t \in [T]} \mathbb{E} \|\nabla f_{\xi_t}(x_t)\|^2 + (c_Q C_a C_{fob})^2 \right),$$

yielding the claim. ■

We are ready to prove the main result, with a learning rate of

$$\gamma = \frac{1}{3(3L_f + C)\sqrt{T}}.$$

PROOF OF THEOREM 3.1: Since  $f$  has  $L_f$ -Lipschitz gradient, we know that

$$f(x_{t+1}) - f(x_t) \leq -\gamma \cdot \langle \nabla f(x_t), g_{\xi_t}(x_t) + \Delta_{\xi_t}(x_t) \rangle + \frac{\gamma^2 L_f}{2} \|g_{\xi_t}(x_t) + \Delta_{\xi_t}(x_t)\|^2.$$

Since the quantization is unbiased, implying  $\mathbb{E}_Q[\Delta_{\xi_t}^{(Q)}(x)] = 0$ , taking the expectation with respect to the quantization yields

$$\begin{aligned} \mathbb{E}_Q[f(x_{t+1})] - \mathbb{E}_Q[f(x_t)] \\ \leq -\gamma \mathbb{E}_Q \langle \nabla f(x_t), g_{\xi_t}(x_t) + \tilde{\Delta}_{\xi_t}(x_t) \rangle + \frac{3\gamma^2 L_f}{2} \left( \|g_{\xi_t}(x_t)\|^2 + \|\tilde{\Delta}_{\xi_t}(x_t)\|^2 + \mathbb{E}_Q \|\Delta_{\xi_t}^{(Q)}\|^2 \right), \end{aligned}$$

where  $\tilde{\Delta}_{\xi_t}(x_t) = (\Delta_{\xi_t}^{(a)}, \Delta_{\xi_t}^{(b)})$ , and we used  $(\alpha + \beta + \rho)^2 \leq 3\alpha^2 + 3\beta^2 + 3\rho^2$ .

Taking the expectation over  $\xi_t$  (simplifying the notation of  $\mathbb{E}_Q \mathbb{E}_\xi$  to simply  $\mathbb{E}$ ), and recalling that  $\mathbb{E}[g_{\xi_t}(x_t)] = \nabla f(x_t)$ , we can bound the first two terms of the RHS by

$$\begin{aligned} & -\gamma \mathbb{E} \langle \nabla f(x_t), g_{\xi_t}(x_t) + \tilde{\Delta}_{\xi_t}(x_t) \rangle + \frac{3}{4} \gamma^2 L_f \mathbb{E} \|g_{\xi_t}(x_t) + \tilde{\Delta}_{\xi_t}(x_t)\|^2 \\ & \leq -\frac{\gamma}{2} \mathbb{E} \|\nabla f(x_t)\|^2 + \frac{\gamma}{2} \mathbb{E} \|\tilde{\Delta}_{\xi_t}(x_t)\|^2 + \frac{3}{2} \gamma^2 L_f \mathbb{E} (\|g_{\xi_t}(x_t)\|^2 + \|\tilde{\Delta}_{\xi_t}(x_t)\|^2) \quad \{\alpha \cdot \beta \leq \frac{1}{2}(\alpha^2 + \beta^2)\} \\ & \leq \left(-\frac{\gamma}{2} + 3\gamma^2 L_f\right) \mathbb{E} \|\nabla f(x_t)\|^2 + \left(\frac{\gamma}{2} + \frac{3}{2} \gamma^2 L_f\right) \mathbb{E} \|\tilde{\Delta}_{\xi_t}(x_t)\|^2 + 3\gamma^2 L_f \sigma^2 \quad \{\mathbb{E} \|g_{\xi_t} - \nabla f\|^2 \leq \sigma^2\} \\ & \leq \left(-\frac{\gamma}{2} + 3\gamma^2 L_f\right) \mathbb{E} \|\nabla f(x_t)\|^2 \\ & \quad + \left(\frac{\gamma}{2} + \frac{3}{2} \gamma^2 L_f\right) (1 + C_a)^2 L_{f_{ob}}^2 \mathbb{E} \|\delta_{\xi_t}(x_t)\|^2 + 3\gamma^2 L_f \sigma^2. \quad \{\text{Lemma A.2}\} \end{aligned}$$

Reorganizing the terms, summing over all  $t \in [T]$  and dividing by  $T$  yields

$$\begin{aligned} & \gamma \cdot \left(\frac{1}{2} - 3\gamma L_f\right) \cdot \frac{1}{T} \sum_{t \in [T]} \mathbb{E} \|\nabla f(x_t)\|^2 \leq \frac{f(x_1) - \mathbb{E}[f(x_{T+1})]}{T} + \gamma \cdot C'' \cdot \frac{1}{T} \sum_{t \in [T]} \mathbb{E} \|\delta_{\xi_t}(x_t)\|^2 \\ & \quad + \gamma^2 L_f (3\sigma^2 + \frac{3}{2} \cdot (c_Q C_a C_{f_{ob}})^2), \end{aligned}$$

where

$$C'' = \left(\frac{1}{2} + \frac{3}{2} \gamma L_f\right) (1 + C_a)^2 L_{f_{ob}}^2 < (1 + C_a)^2 L_{f_{ob}}^2, \quad (\text{A.1})$$

by the definition of  $\gamma$ . Applying Lemma A.2 and regrouping the terms now yields

$$\begin{aligned} & \gamma \cdot \left(\frac{1}{2} - 3\gamma L_f - \gamma^2 \cdot C' C''\right) \cdot \frac{1}{T} \sum_{t \in [T]} \|\nabla f(x_t)\|^2 \\ & \leq \frac{f(x_1) - \mathbb{E}[f(x_{T+1})]}{T} + \gamma^2 (\gamma \cdot C' C'' + 3L_f) \cdot (\sigma^2 + (c_Q C_a C_{f_{ob}})^2). \end{aligned}$$

Noting that  $C' C'' < C^2$  and recalling that  $\gamma C < 1/3$  and  $\gamma L_f < 1/9$ , we get

$$\begin{aligned} & \gamma \cdot \left(\frac{1}{2} - \gamma(3L_f + C)\right) \cdot \frac{1}{T} \sum_{t \in [T]} \|\nabla f_{\xi_t}(x_t)\|^2 \\ & \leq \frac{f(x_1) - \mathbb{E}[f(x_{T+1})]}{T} + \gamma^2 (3L_f + C) \cdot (\sigma^2 + (c_Q C_a C_{f_{ob}})^2). \end{aligned}$$

Since  $\gamma \cdot (3L_f + C) = \frac{1}{3\sqrt{T}} \leq \frac{1}{3}$ , the LHS coefficient is at least  $\gamma/6$ , so dividing by  $\gamma/6$  now yields the claim by substituting  $\gamma$  with  $\frac{1}{3(3L_f + C)\sqrt{T}}$ .  $\blacksquare$

## A.1 Theoretical analysis when $K > 2$

In this section we sketch how one can generalize the already provided theoretical analysis for the  $K = 2$  case.

Instead of Machines  $a$  and  $b$ , we now suppose that we have a stack  $a_1, \dots, a_K$  of  $K$  Machines such that every pair  $a_i, a_{i+1}$  communicates a compressed message, denoted by  $m_i$ . We simplify the notation of the complete model by  $x = (x^{(1)}, \dots, x^{(K)})$ , and, for a sample  $\xi$ , further denote

$$\bar{a}^{(i)}(\xi, x_t) = a_i(a_{i-1}(\dots(a_1(\xi, x_t^{(1)}), x_t^{(2)}), \dots, x_t^{(i)})),$$

$$\bar{m}^{(i)}(\xi, x_t) = m_i(m_{i-1}(\dots(m_1(\xi, x_t^{(1)}), x_t^{(2)}), \dots, x_t^{(i)})),$$

for  $i \in [K]$ . As in Algorithm 1, for iteration  $t$  and the data sample  $\xi_t$ , if it is the first time that  $\xi_t$  is sampled, Machine  $a_i$  communicates to Machine  $a_{i+1}$  the full precision activations without any compression:  $m_i(\xi_t) = \bar{a}^{(i)}(\xi_t, x_t)$ . If  $\xi_t$  has been sampled in previous iterations, Machine  $a_i$  communicates a compressed version:

$$Q(a_i(\bar{m}^{(i-1)}(\xi_t), x_t^{(i)}) - m_i(\xi_t)),$$

where  $m_i(\xi_t)$  was the previous message, stored in the local buffer. Both machines then update this local buffer:

$$m_i(\xi_t) \leftarrow m_i(\xi_t) + Q(a_i(\bar{m}^{(i-1)}(\xi_t), x_t^{(i)}) - m_i(\xi_t)).$$

Machine  $a_{i+1}$  then uses  $m_i(\xi_t)$  as the forward activations. Upon receiving backward gradients from Machine  $a_{i+2}$ , it computes backward gradients, and communicates a quantized version of the backward gradient to Machine  $a_i$ . We use

$$\delta_\xi^{(i)} = \bar{a}^{(i)}(\xi, x_t) - \bar{m}^{(i)}(\xi, x_t)$$

to denote the *message error* of  $i$ -th machine in sending the activations (accumulated also through messages in previous pairs), and denote the *total message error* by  $\delta_\xi = (\delta_\xi^{(1)}, \dots, \delta_\xi^{(K-1)})$ .

**Update Rules.** We can now generalize the update rule for  $a$  and  $b$  to

$$x_{t+1}^{(K)} = x_t^{(K)} - \gamma \cdot \nabla_{x^{(K)}}(f \circ a_K) \big|_{(\bar{m}^{(K-1)}(\xi_t), x_t^{(K)})},$$

$$x_{t+1}^{(i)} = x_t^{(i)} - \gamma \cdot Q(\nabla_{a_i}(f \circ a_K \circ \dots \circ a_{i+1}) \big|_{(\bar{m}^{(i)}(\xi_t), x_t^{(i+1)}, \dots, x_t^{(K)})}) \cdot \nabla_{x^{(i)}} a_i \big|_{(\bar{m}^{(i-1)}(\xi_t), x_t^{(i)})},$$

for  $i=1, \dots, K-1$ , where  $\gamma$  is the learning rate. We can rephrase the update rule as

$$x_{t+1} = x_t - \gamma \cdot (g_\xi(x_t) + \Delta_\xi(x_t)),$$

where  $g_\xi(x_t)$  is the stochastic gradient and  $\Delta_\xi(x_t)$  is the *total gradient error* introduced by communication compression. We have  $\Delta_\xi = (\Delta_\xi^{(1)} + \Delta_\xi^{(Q,1)}, \dots, \Delta_\xi^{(K-1)} + \Delta_\xi^{(Q,K-1)}, \Delta_\xi^{(K)})$ , given by:

$$\begin{aligned} \Delta_\xi^{(Q,i)}(x_t) &= Q(\nabla_{a_i}(f \circ a_K \circ \dots \circ a_{i+1}) \big|_{(\bar{m}^{(i)}(\xi_t), x_t^{(i+1)}, \dots, x_t^{(K)})}) \cdot \nabla_{x^{(i)}} a_i \big|_{(\bar{m}^{(i-1)}(\xi_t), x_t^{(i)})} \\ &\quad - \nabla_{a_i}(f \circ a_K \circ \dots \circ a_{i+1}) \big|_{(\bar{m}^{(i)}(\xi_t), x_t^{(i+1)}, \dots, x_t^{(K)})} \cdot \nabla_{x^{(i)}} a_i \big|_{(\bar{m}^{(i-1)}(\xi_t), x_t^{(i)})}, \end{aligned}$$

$$\begin{aligned} \Delta_\xi^{(i)}(x_t) &= \nabla_{a_i}(f \circ a_K \circ \dots \circ a_{i+1}) \big|_{(\bar{m}^{(i)}(\xi_t), x_t^{(i+1)}, \dots, x_t^{(K)})} \cdot \nabla_{x^{(i)}} a_i \big|_{(\bar{m}^{(i-1)}(\xi_t), x_t^{(i)})} \\ &\quad - \nabla_{a_i}(f \circ a_K \circ \dots \circ a_{i+1}) \big|_{(\bar{a}^{(i)}(\xi_t), x_t^{(i+1)}, \dots, x_t^{(K)})} \cdot \nabla_{x^{(i)}} a_i \big|_{(\bar{a}^{(i-1)}(\xi_t), x_t^{(i)})}, \end{aligned}$$

$$\Delta_\xi^{(K)}(x_t) = \nabla_{x^{(K)}}(f \circ a_K) \big|_{(\bar{m}^{(K-1)}(\xi_t), x_t^{(K)})} - \nabla_{x^{(K)}}(f \circ a_K) \big|_{(\bar{a}^{(K-1)}(\xi_t), x_t^{(K)})},$$

for all  $i=1, \dots, K-1$ .

**Generalized Assumptions.** In order to state the analogue of Theorem 3.1 for  $K > 2$ , we need to define the corresponding assumptions with respect to Lipschitz properties (whereas Assumption GA2 is here only for completeness, being the same as A2).

- **(GA1: Lipschitz assumptions)** We assume that
  - $f$  had  $L_f$ -Lipschitz gradient,
  - $f \circ a_K \circ \dots \circ a_{i+1}$  has  $L_{f \circ a_K \circ \dots \circ a_{i+1}}$ -Lipschitz gradient, and has gradient bounded by  $C_{f \circ a_K \circ \dots \circ a_{i+1}}$  for all  $i=1, \dots, K-1$ ,
  - $a_i$  is  $\ell_{a_i}$ -Lipschitz, and has gradient bounded by  $C_{a_i}$ , for all  $i=1, \dots, K$ .
- **(GA2: SGD assumptions)** We assume that the stochastic gradient  $g_\xi$  is unbiased, i.e.  $\mathbb{E}_\xi[g_\xi(x)] = \nabla f(x)$ , for all  $x$ , and with bounded variance, i.e.  $\mathbb{E}_\xi\|g_\xi(x) - \nabla f(x)\|^2 \leq \sigma^2$ , for all  $x$ .

We have the following analogue of Theorem 3.1.

**Theorem A.3.** Suppose that Assumptions GA1, GA2 hold, and let

$$\tilde{C} = \sqrt{\sum_{i=1}^{K-1} C_{a_i}^2 C_{f \circ a_K \circ \dots \circ a_{i+1}}^2}.$$

Consider an unbiased quantization function  $Q(x)$  which satisfies that there exists  $c_Q < \sqrt{1/2}$  such that  $\mathbb{E}\|x - Q(x)\| \leq c_Q\|x\|$ , for all  $x$ . Then there exists a constant  $C$  that depends only on the constants defined above and on  $\sqrt{K}$  and  $N$ , such that for the learning rate  $\gamma$  proportional to  $\frac{1}{(C+L_f)\sqrt{T}}$ , after performing  $T$  updates one has

$$\frac{1}{T} \sum_{t \in [T]} \mathbb{E}\|\nabla f(x_t)\|^2 \lesssim \frac{(C+L_f)(f(x_1) - f^*)}{\sqrt{T}} + \frac{\sigma^2 + (c_Q \tilde{C})^2}{\sqrt{T}}. \quad (\text{A.2})$$

Instead of performing a tedious job of rewriting the proof of the  $K = 2$  case with inherently more constant-chasing, we will simply sketch the differences with respect to the proof of Theorem 3.1. First we note that, having analogous assumptions as in the case when  $K = 2$ , we can easily prove the following analogue of Lemma A.1.

**Lemma A.4.** *Let*

$$\Delta_\xi^{(Q)} = (\Delta_\xi^{(Q,1)}, \dots, \Delta_\xi^{(Q,K-1)}).$$

*For every sample  $\xi$ , one has*

$$\|\Delta_\xi^{(Q,i)}(x)\| \leq c_Q C_{a_i} C_{f \circ a_K \circ \dots \circ a_{i+1}}, \quad i = 1, \dots, K-1,$$

$$\|\Delta_\xi^{(i)}(x)\| \leq C_{a_i} L_{f \circ a_K \circ \dots \circ a_{i+1}} \|\delta_\xi^{(i)}\| + C_{f \circ a_K \circ \dots \circ a_{i+1}} L_{a_i} \|\delta_\xi^{(i-1)}\|, \quad i = 1, \dots, K-1,$$

*and*

$$\|\Delta_\xi^{(K)}(x)\| \leq L_{f \circ a_K} \|\delta_\xi^{(K-1)}\|,$$

*implying  $\|\Delta_\xi^{(Q)}\| \leq \tilde{C} c_Q$ .*

Comparing this with Lemma A.1, we see that for  $\tilde{\Delta}_\xi = (\Delta_\xi^{(1)}, \dots, \Delta_\xi^{(K)})$ , we now have an additional term that depends on  $\delta_\xi^{(i-1)}$ . However, since in the proof of Theorem 3.1 we only rely on  $\|\Delta_\xi\|^2$ , we can proceed even with a crude bound

$$\begin{aligned} \|\tilde{\Delta}_\xi\|^2 &= \sum_{i=1}^K \|\Delta_\xi^{(i)}\|^2 \\ &\leq (1 + 2C_{a_{K-1}}^2) L_{f \circ a_K}^2 \|\delta_\xi^{(K-1)}\|^2 + 2 \sum_{i=1}^{K-2} (C_{a_{K-2}}^2 L_{f \circ a_K \circ \dots \circ a_{i+1}}^2 + C_{f \circ a_K \circ \dots \circ a_{i+2}}^2 L_{a_{i+1}}^2) \|\delta_\xi^{(i)}\|^2 \\ &\leq 2K \cdot \underbrace{\max \left\{ (1 + 2C_{a_{K-1}}^2) L_{f \circ a_K}^2, \max_{i \in [K-2]} \{ C_{a_{K-2}}^2 L_{f \circ a_K \circ \dots \circ a_{i+1}}^2 + C_{f \circ a_K \circ \dots \circ a_{i+2}}^2 L_{a_{i+1}}^2 \} \right\}}_{C_1} \|\delta_\xi\|^2. \end{aligned}$$

Mimicking closely the steps of Lemma A.2, separately for each  $i$  and the summing over all  $i$  via  $\|\ell_a\|^2 = \sum_{i=1}^K \|\ell_{a_i}\|^2$ , one can straightforwardly yield the following analogue of Lemma A.2.

**Lemma A.5.** *For  $C' = K \cdot \frac{36c_Q^2 \|\ell_a\|^2 N^2 C_1}{1 - 2c_Q^2}$ , where  $\ell_a = (l_{a_1}, \dots, l_{a_K})$ , one has*

$$\frac{1}{T} \sum_{t \in [T]} \mathbb{E} \|\delta_{\xi_t}(x_t)\|^2 \leq C' \gamma^2 \cdot \left( \frac{1}{T} \sum_{t \in [T]} \mathbb{E} \|\nabla f(x_t)\|^2 + \sigma^2 + (c_Q \tilde{C})^2 \right).$$

Theorem A.3 can now be proved by repeating the steps of the proof of Theorem 3.1, carefully substituting Lemma A.1 by Lemma A.4, and Lemma A.2 by Lemma A.5.

Dataset	# labels	# train samples	Task description
QNLI	2	105K question-paragraph pairs	natural language inference
CoLA	2	8.6K sentences	linguistic acceptability
WikiText2	-	2M tokens	language modeling
arXiv	-	7M tokens	language modeling

Table 3: Dataset statistics

## B Benchmark Dataset

The data statistics can be found in Table 3. We fine-tune DeBERTa on QNLI and CoLA datasets. The QNLI task is to determine whether the context sentence contains the answer to the question. The CoLA task aims to detect whether a given sequence of tokens is a grammatical English sentence. In addition, we fine-tune GPT2 on the WikiText2 training set. We also collect 30K arXiv abstracts in 2021 to fine-tune GPT2. Neither corpus is included in the GPT2 pre-training data set.

## C Training Task Setup and Hyper-parameter Tuning

**Sequence Classification.** We use the AdamW optimizer to fine-tune the model for 10 epochs. Specifically, for QNLI, we set the learning rate to 3.0e-6, learning rate warm-up steps to 1000, max sequence length to 256, the macro-batch size to 64 and micro-batch size to 8; for CoLA, we set the learning rate to 2.5e-6, learning rate warm-up steps to 250, max sequence length to 128, the macro-batch size to 32 and micro-batch size to 8. After the learning rate warm-up stage, we decay the learning rate linearly over the training epochs.

**Language Modeling.** For both WikiText and arXiv datasets, we use AdamW optimizer with a learning rate of 5.0e-6. We train the model for 10 epochs with a macro-batch size of 32 and a micro-batch size of 1. The max sequence length is set to 1024 for both datasets. After the learning rate warm-up stage, we decay the learning rate linearly over the training epochs.

## D Distributed View of AC-SGD Algorithm

Algorithm 2 shows a multi-node view of AC-SGD. For brevity, we omit the first warm-up epoch, where we conduct uncompressed training, and thus we update the previous messages by  $m(\xi) \leftarrow a(\xi, x)$ .

## E Additional Results

We provide additional experimental results. Specifically, we show:

- the convergence results with standard deviation;
- the training throughput for different dataset settings;
- the robustness of AC-SGD under different hyperparameter settings;
- the effectiveness of AC-SGD in the split learning scenario.

### E.1 Convergence Results with Standard Deviation

In the main content, we show the convergence performance of different approaches. We repeated each experiment three times to ensure reproducibility. We calculate the moving averages of these convergence curves and then average the results of repeated experiments. We visualize (shaded areas) the moving standard deviation in all repeated experiments in Figure 6. Overall, we observe consistent results for all datasets.

---

**Algorithm 2** AC-SGD Algorithm

---

**Initialize:**  $x_0$ , learning rate  $\gamma$ , network  $a$ 's weights  $x^{(a)}$ , network  $b$ 's weights  $x^{(b)}$ , quantization function  $Q$ , the arrays of previous messages  $m$ , where networks  $a$  and  $b$  each maintain a copy of it.

**for**  $t = 1, \dots, T$  **do**

**(on network  $a$ )**

        Randomly sample  $\xi_t$

$\Delta m(\xi_t) \leftarrow Q(a(\xi_t, x_t^{(a)}) - m(\xi_t))$

        Update  $m(\xi_t) \leftarrow m(\xi_t) + \Delta m(\xi_t)$

        Send  $\Delta m(\xi_t)$  to network  $b$

**(on network  $b$ )**

        Update  $m(\xi_t) \leftarrow m(\xi_t) + \Delta m(\xi_t)$

        Update  $x_{t+1}^{(b)} \leftarrow x_t^{(b)} - \gamma \cdot \nabla_{x^{(b)}}(f \circ b)|_m$

        Send  $Q(\nabla_a(f \circ b)|_m)$  to network  $a$

**(on network  $a$ )**

        Update  $x_{t+1}^{(a)} \leftarrow x_t^{(a)} - \gamma \cdot Q(\nabla_a(f \circ b)|_m) \cdot \nabla_{x^{(a)}} a$

**end for**

**Output:**  $x = (x_T^{(a)}, x_T^{(b)})$

---

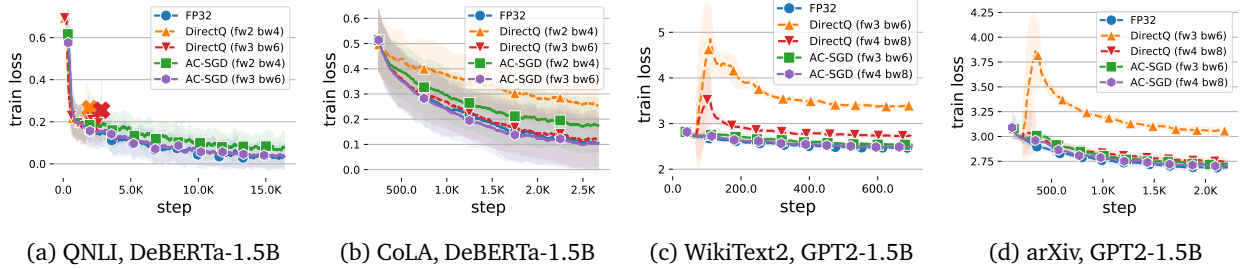


Figure 6: Convergence (loss vs. # steps) of different approaches.  $\times$  represents divergence.

## E.2 Throughput under Different Dataset Settings

We show the training throughput under different dataset settings in Figure 4. In general, the observation is similar to that of the main content: our approach maintains similar throughput even when the network is  $100\times$  slower (from 10Gbps to 100Mbps). WikiText2 and arXiv have essentially the same throughput results, since we use the same training settings for them.

## E.3 Hyper-parameter Sensitivity

Here we demonstrate the robustness of our method in various settings. For fast validation, we focus on evaluating DeBERTa-v3-base<sup>4</sup> on QNLI and CoLA datasets. We by default use  $K = 4$  devices for pipeline parallel training, 2 bits for forward activation, and 4 bits for backward gradients (fw2 bw4).

**Number of Pipeline Stages.** We first investigate the influence of the number of pipeline stages on convergence performance. Intuitively, partitioning into more pipeline stages leads to more rounds of data compression and communication, resulting in a larger accumulated compression error. The results of Figures 7a and 7b confirm this intuition. Specifically, the direct quantization method works not bad when  $K = 2$ , but its performance becomes unsatisfied when we further enlarge  $K$ . In comparison, our approach can maintain similar convergence performance to FP32.

<sup>4</sup><https://huggingface.co/microsoft/deberta-v3-base>

Table 4: Training Throughput.

Network Bandwidth	DeBERTa-1.5B, QNLI			GPT2-1.5B, WikiText2		
	FP32	DirectQ fw2 bw4 / fw3 bw6	AC-SGD fw2 bw4 / fw3 bw6	FP32	DirectQ fw3 bw6 / fw4 bw8	AC-SGD fw3 bw6 / fw4 bw8
10 Gbps	12.9 $\pm$ 0.02	13.6 $\pm$ 0.02 / 13.6 $\pm$ 0.02	13.6 $\pm$ 0.02 / 13.5 $\pm$ 0.02	3.8 $\pm$ 0.01	4.0 $\pm$ 0.01 / 4.1 $\pm$ 0.01	4.0 $\pm$ 0.01 / 4.0 $\pm$ 0.01
1 Gbps	9.6 $\pm$ 0.02	13.3 $\pm$ 0.02 / 13.1 $\pm$ 0.02	13.3 $\pm$ 0.02 / 13.0 $\pm$ 0.02	3.2 $\pm$ 0.01	4.0 $\pm$ 0.01 / 4.0 $\pm$ 0.01	4.0 $\pm$ 0.01 / 3.9 $\pm$ 0.01
500 Mbps	6.2 $\pm$ 0.03	13.0 $\pm$ 0.03 / 12.6 $\pm$ 0.03	12.9 $\pm$ 0.03 / 12.5 $\pm$ 0.03	2.7 $\pm$ 0.02	3.9 $\pm$ 0.01 / 3.9 $\pm$ 0.01	3.9 $\pm$ 0.01 / 3.9 $\pm$ 0.01
300 Mbps	4.4 $\pm$ 0.04	12.5 $\pm$ 0.02 / 11.9 $\pm$ 0.03	12.4 $\pm$ 0.03 / 11.8 $\pm$ 0.03	1.8 $\pm$ 0.02	3.9 $\pm$ 0.01 / 3.8 $\pm$ 0.01	3.8 $\pm$ 0.01 / 3.8 $\pm$ 0.01
100 Mbps	1.6 $\pm$ 0.04	10.7 $\pm$ 0.03 / 9.4 $\pm$ 0.03	10.6 $\pm$ 0.03 / 9.1 $\pm$ 0.03	0.5 $\pm$ 0.02	3.5 $\pm$ 0.02 / 3.0 $\pm$ 0.02	3.4 $\pm$ 0.01 / 3.0 $\pm$ 0.02

Network Bandwidth	DeBERTa-1.5B, CoLA			GPT2-1.5B, arXiv		
	FP32	DirectQ fw2 bw4 / fw3 bw6	AC-SGD fw2 bw4 / fw3 bw6	FP32	DirectQ fw3 bw6 / fw4 bw8	AC-SGD fw3 bw6 / fw4 bw8
10 Gbps	17.1 $\pm$ 0.03	18.0 $\pm$ 0.03 / 17.9 $\pm$ 0.03	17.9 $\pm$ 0.03 / 17.8 $\pm$ 0.03	3.8 $\pm$ 0.01	4.0 $\pm$ 0.01 / 4.1 $\pm$ 0.01	4.0 $\pm$ 0.01 / 4.0 $\pm$ 0.01
1 Gbps	12.2 $\pm$ 0.03	17.4 $\pm$ 0.02 / 17.1 $\pm$ 0.02	17.3 $\pm$ 0.02 / 16.9 $\pm$ 0.02	3.2 $\pm$ 0.01	4.0 $\pm$ 0.01 / 4.0 $\pm$ 0.01	4.0 $\pm$ 0.01 / 3.9 $\pm$ 0.01
500 Mbps	8.9 $\pm$ 0.03	16.7 $\pm$ 0.03 / 16.2 $\pm$ 0.03	16.7 $\pm$ 0.03 / 16.1 $\pm$ 0.03	2.7 $\pm$ 0.02	3.9 $\pm$ 0.01 / 3.9 $\pm$ 0.01	3.9 $\pm$ 0.01 / 3.9 $\pm$ 0.01
300 Mbps	6.0 $\pm$ 0.04	16.1 $\pm$ 0.03 / 15.2 $\pm$ 0.03	16.0 $\pm$ 0.03 / 15.1 $\pm$ 0.03	1.8 $\pm$ 0.02	3.9 $\pm$ 0.01 / 3.8 $\pm$ 0.01	3.8 $\pm$ 0.01 / 3.8 $\pm$ 0.01
100 Mbps	2.2 $\pm$ 0.04	13.1 $\pm$ 0.03 / 11.5 $\pm$ 0.03	13.1 $\pm$ 0.03 / 11.3 $\pm$ 0.03	0.5 $\pm$ 0.03	3.5 $\pm$ 0.01 / 3.0 $\pm$ 0.02	3.4 $\pm$ 0.01 / 3.0 $\pm$ 0.01

**Number of Bits in Communication.** Figures 7c and 7d compare different methods with different numbers of bits in communication. We observe that using more bits can improve the convergence performance but lead to higher communication overheads. In general, our approach achieves better accuracy-efficiency trade-offs.

**Number of Bits for Previous Messages.** We may find that storing all previous messages is space-intensive. To reduce such requirements, we show that previous messages  $m$  can be preserved with low precision. We here perform quantization on  $m$ , where  $mz$  means that we use  $z$  bits for previous messages. Figures 7e and 7f show the results with different number of bits of the previous messages. When only 2 bits are used for the previous messages, despite the fact that it is slightly worse than our default setting, our approach is still significantly better than DirectQ. And there is no significant performance drop when 8 bits are used for the previous messages.

**Pre-trained Model Sizes.** Figures 7g and 7h show the results of the base and large version of DeBERTa. Surprisingly, larger models seem to be more tolerant of errors from activation compression than smaller models. One possible reason is that larger models usually use much smaller learning rates. So the error of each iteration can be restricted to a smaller range. Here, we use  $2.0e-5$  for the base model and  $7e-6$  for the large model, as suggested in the official repository of DeBERTa.

## E.4 Split Learning

Split learning is a scenario of federated learning, where the client trains a shallow part of deep network (known as the cut layer) that accesses the training data, while the rest of the model is trained in a data center. Clients and server need to exchange the activation and its gradients in the cut, where AC-SGD can be adopted. We evaluated AC-SGD on a split learning scenario where neither the input data nor its labels are shared with the server—the model is cut twice, one after the first resnet block and one before the last block to generate the prediction. We evaluate AC-SGD for split learning over Cifar10 and Cifar100 with the ResNet34 model. We set 16 clients and use a Dirichlet distribution with concentration parameter 0.5 to synthesize non-identical datasets. Following the previously established work of split learning, in each communication round, we conduct local training for each client sequentially, and each client will train 3 epochs with its local data. We utilize SGD optimizer with momentum of 0.9, a batch size of 64, and a learning rate of 0.01. We decay the learning rate to its 10% for every 20 communication rounds.

The datasets are augmented with random cropping and flipping. To adapt to random cropping, we do the same cropping operation on the retrieved previous message, and only update its non-cropped part. To adapt to random flipping, we maintain another previous message copy for flipped images, and retrieve and update only the corresponding copy during training.

Figure 8 presents the results of split learning, where fw2 bw8[0.2] means that, for forward pass, we

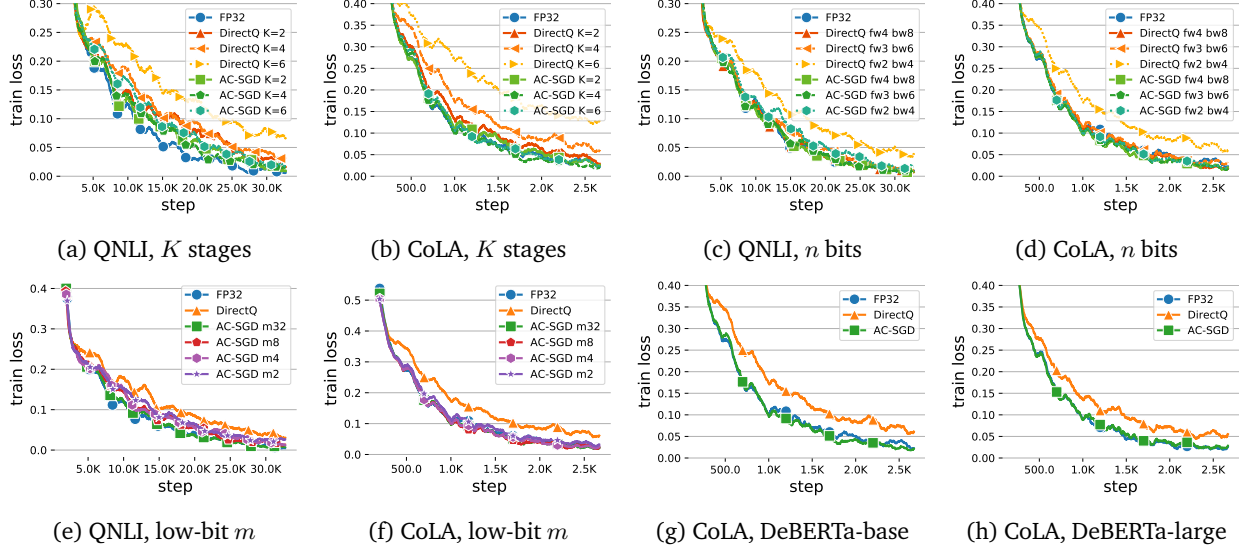


Figure 7: Convergence curves under different configurations.

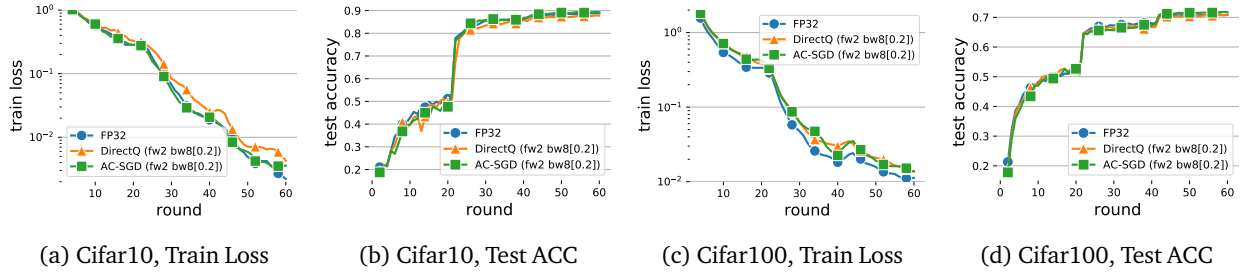


Figure 8: Results of split learning with ResNet34.

perform 2-bit quantization, and for backward pass, we keep only the top 20% gradients and then perform 8-bit quantization. We can see that AC-SGD transfers the activations in 2 bits while maintaining a performance similar to FP32, which indicates the effectiveness of AC-SGD in improving the communication efficiency in the split learning scenario. Furthermore, compared to DirectQ, AC-SGD shows advantages in terms of both the convergence and generalization of the trained model.